PPPL--1894

DE92 016000

Estimated Neutron-Activation Data for TFTR

Part II.

Biological Dose Rate from Sample-Material Activation

Long-poe Ku and J. G. Kolibal

DISCLAIMER

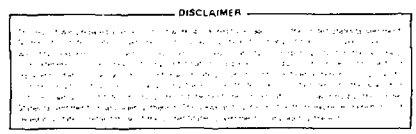

Princeton Plasma Physics Laboratory

Princeton, New Jersey 08544

DISTRIBUTION OF THIS DOCUMENT IS UNLIMITED

TABLE ON CONTENTS

ABSTRACT

The neutron induced material activation dose rate data are summarized for the TFTR operation. This report marks the completion of the second phase of the systematic study of the activation problem on the TFTR (See Ref. 1 for the details of the sequence of study).

The estimations of the neutron induced activation dose rates were made for spherical and slab objects, based on a point kernel method, for a wide range of materials. The dose rates as a function of cooling time for standard samples are presented for a number of typical neutron spectrum expected during TFTR DD and DT operations. The factors which account for the variations of the pulsing history, the characteristic size of the object and the distance of observation relative to the standard samples are also presented.

I. INTRODUCTION

In Part I of this report, the importance of having a systematic study of the neutron induced activation on the TFTR has been described (Ref. 1). The fundamental data and the formulae for calculating the specific radioactivities have also been given. Part II summarizes the dose rate data for some sample materials relevant to the TFTR operation.

The dose rate is a direct measure of the biological impact of an activated object, thus it is an essential piece of information affecting the methods used to disassemble and handle activated equipment. When an object is small, the dose rate decreases rapidly from the surface of the object ($1/r^{**}2$), so that the effect on the dose rate field due to the presence of this object is localized. However, this localized effect can still dominate the global dose field close to the object. Since it is virtually impossible to include all the materials in the calculation of the global dose field, the local contribution to the existing dose field may be best estimated by examining the dose rate from those individual objects which have not been included in the global modeling. A compilation of the activation data from a wide range of materials has a further application. It allows an understanding of the characteristics of the material activation properties in a DD and DT fusion neutron environment, thus allowing a comparative selection of materials based on their activation characteristics.

The dose rate data for sample materials were derived using a point kernel method, that is the dose rate was calculated by integrating the uncollided contribution of the radiation over the source volume. The details of the radiation transport were implicit in such calculations, and were described by dose build-up factors. The method is rapid, practical, and generally yields satisfactory results. For engineering applications, any odd shaped object may be regarded as the union and intersection of simple bodies for which explicit dose rate equations have been derived. Such an approach, of course, overlooks the affect of self shielding to some extent; however, provided the objects are not too large considered together, these errors will add only slightly to the conservatism of the results. A system by which a user can derive the

dose rate as desired, especially for spherical and slab geometries is provided.

For a given configuration of objects, the activation dose rate depends on the material composition, the prompt neutron field strength, the spectral shape of the neutron flux, the cooling time, the irradiation history, the size of the object and the distance of the observer from the object. To characterize the data and to make it manageable, the dose rates due to standard samples material were calculated for a set of nominal materials, along with a set of factors which account for the time, size and distance. Materials were chosen which were representative in terms of usage and activation of the many materials used in the construction of the TFTR. The samples ranged from typical Cr-Fe-Ni alloys to solders and brazes.

In the following presentation, Section 2 summarizes the methods and basic equations used. Section 3 is a discussion of the assumptions involved and their validity. Section 4 gives the standard sample activation data and the important isotopes contributing to the dose rate. Section 5 discusses the factors which account for the pulsing history, the size of the object and the observation distance. Section 6 illustrates how to extend the application of the compiled data, and some sample problems are shown.

II. METHODOLOGY

The estimate of the dose rate was made using point kernel integration, which can be written as

$$D(\vec{r}, t_w) = \int_{V_s} \int_E S(\vec{r}', E', t_w)\, k(\lambda, |\vec{r}-\vec{r}'|, E') \cdot C(E')\, dE'\, d V_s, \qquad (1)$$

where

$D(\vec{r}, t_w)$ = dose rate at location $\vec{r}$ and cooling time t_w.

$S(\vec{r}', E', t_w)$ = residual gamma-ray strength at location $\vec{r}'$, with energy E' and at cooling time t_w.

$k(\lambda, |\vec{r}-\vec{r}'|, E')$ = gamma-ray attenuation kernel for a point source at $\vec{r}'$ and a detector at $\vec{r}$ for a total attenuation mean-free-path λ.

$$= \frac{e^{-\lambda} B(\lambda, E', Z)}{4\pi (\vec{r}-\vec{r}')^2} \qquad (2)$$

$C(E)$ = photon flux to dose rate conversion factor.

$B(\lambda, E', Z)$ = dose build-up factor

$$= \frac{\text{total dose rate}}{\text{uncollided dose rate}}$$

for gamma-rays with energy E', attenuated by a medium of thickness λ mean-free-paths (mfp) and having an effective atomic number Z.

V_s = residual gamma-ray source volume.

If we assume that the source strength is uniform, it can be shown that, without an external shield, for an infinite slab of thickness a,

$$D(\vec{r}, t_w) = \int_E \frac{S_v(E', t_w) C(E')}{2} \sum_{i=1}^{2} \frac{A_i a}{(1+\alpha_i)\lambda_a} \cdot \{1 - E_2[(1+\alpha_i)\lambda_a]\} dE' , \qquad (3)$$

and for a sphere of radius a,

$$D(\vec{r}, t_w) = \int_E \frac{S_v(E', t_w) C(E')}{2} \sum_{i=1}^{2} \frac{A_i a}{(1+\alpha_i)\lambda_a} \cdot [1 - \cos\theta][1 - e^{-\beta_i}] dE' \qquad (4)$$

where,

$S_v(E, t_w)$ = residual gamma-ray strength per unit volume.

λ_a = total mean-free-path for radiation traversing a thickness a

$= \mu a$

μ = total linear attenuation coefficient

$$\theta = \sin^{-1} \frac{a}{r_o + a} \tag{5}$$

r_o = detector distance measured from the surface of a sphere.

$$\beta_i = m_s \left(1 + \alpha_i\right) \lambda_a \tag{6}$$

$$m_s = \left[\frac{2}{1 - \cos\theta} + \left(\frac{r_o}{a}\right)^3\right]^{1/3} - \left(\frac{r_o}{a}\right) \tag{7}$$

E_2 = exponential integral function

The Taylor-form of the dose build-up factor (Ref. 2) has been used in the above equations. That is

$$B\left(\lambda, E', Z\right) = A_1 e^{-\alpha_1 \lambda} + A_2 e^{-\alpha_2 \lambda} \tag{8}$$

$$A_2 = 1 - A_1 \tag{9}$$

where A1, α_1 and α_2 are the fitting parameters which depend on the energy of the gamma-rays, E', the atomic number Z of the medium, and the source-detector geometric configuration.

Equations (3) and (4) are the fundamental equations which have been used to generate the activation dose rate data. Equation (3) is mathematically exact. Equation (4) was based on Ono and Tsuruo's work (Ref. 3). According to the authors, the differences are less than ±10% for nearly all values of λ_t, λ_a, and r_o/a where these terms refer to the mfp in external shield, the mfp in the source region, the ratio of the distance from the surface to the radius of the sphere.

For the purpose of correlating the pulsing history, the characteristic size of the sample and the distance of observation, the dose rate for a sample of size, a, at cooling time t_w can be written as

$$D\left(\vec{r},\ t_w;\ n_p,\ a,\ r'\right) = D\left(\vec{r}_o,\ t_w;\ n_{po},\ a_o,\ r'\right)\ \phi_n(\vec{r}')\ f_p\ f_s\ f_d \qquad (10)$$

where,

$D\left(\vec{r},\ t_w;\ n_p,\ a,\ r'\right)$ = dose rate at location $\vec{r}$, cooling time t_w given a sample of size a, located at $\vec{r}'$ and irradiated by n_p pulses. The total neutron flux level at $\vec{r}'$ is normalize to 1 and,

$\phi_n\left(\vec{r}'\right)$ = the magnitude of the neutron flux level.

$$f_p = \frac{D\left(\vec{r}_o,\ t_w;\ n_p,\ a_o,\ \vec{r}'\right)}{D\left(\vec{r}_o,\ t_w;\ n_{po},\ a_o,\ \vec{r}'\right)} \qquad (11)$$

$$f_s = \frac{D\left(\vec{r}_o,\ t_w;\ n_p,\ a,\ \vec{r}'\right)}{D\left(\vec{r}_o,\ t_w;\ n_p,\ a_o,\ \vec{r}'\right)} \qquad (12)$$

$$f_d = \frac{D\left(\vec{r},\ t_w;\ n_p,\ a,\ \vec{r}'\right)}{D\left(\vec{r}_o,\ t_w;\ n_p,\ a,\ \vec{r}'\right)} \ . \qquad (13)$$

Thus $D(\vec{r}_o,\ t_w;\ n_{po},\ a_o,\ \vec{r}')$ is the dose rate due to a standard sample at location $\vec{r}'$ at cooling time t_w. The factors f_p, f_s, and f_d correlate the actual dose rate of a sample to that of the standard sample, taking into account the variations of the pulsing history, the characteristic size and the distance of observation.

In this report, the standard sample was defined as a 0.0127-m-radius sphere; the dose rate due to the standard sample was the surface dose

rate after a sequence of 100 consecutive pulses TFTR baseline operation. Each pulse has been assumed to be 0.5 seconds long, and repeated every 5 minutes.

In deriving the decay gamma-ray strength, the TFTR was divided into 8 areas for which typical neutron spectra were generated (Ref. 1). The following notations for these typical spectra will be used throughout the presentation.

S2: The spectrum at the TFTR vaccum vessel due to DT neutrons;

S3: the spectrum at the TFTR test cell center, without igloo shield, due to DT neutrons;

S4: the spectrum for DT neutrons attenuated by a 0.66-m Limestone concrete shield with a borated concrete reflector behind the shield;

S5: the same as S4, except that the shield thickness has been increased to 0.86 m;

S6: the spectrum for DT neutrons attenuated by a 1.83 m of Limestone concrete shield with an ordinary concrete reflector behind the shield;

S8: the same as S2, except for DD neutrons;

S9: the same as S3, except for DD neutrons; and,

S10: the same as S6 except for DD neutrons.

The distributions for these neutron spectra may be found in Ref. 1, Figs. 2 and 3. Notice that there were no DT burns assumed in a DD pulse.

As mentioned previously, a modular computing system has been established to carry out the dose rate calculation. Following is a brief description of the system and the sequence through which the modules have been executed in the calculation of material activation data.

(1) SPAC module: This generates a specific activity library upon the user's specification of the neutron flux spectrum, the duration and the repetition rate of a pulse, the number of pulses and the cooling time. The SPAC code calculates the specific activity

based on the formula given in Ref. 1 along with the activation cross section library and the isotope decay chain sequence.

(2) DECAL module: This generates a decay gamma-ray data library suitable for later dose rate calculation. The DECAL code incorporates the mass attenuation coefficients, the dose build-up factors, isotope gamma-ray decay intensities and energies into a library (DRAPKILIB) which tabulates the data in such a way that interpolation may be used in the dose rate calculation. Currently, there are about 400 radioactive nuclides whose decay data have been built into the DRAPKILIB. The radiation data were taken from Reference 4, and the attenuation and build-up factor data taken from Reference 5. Note that only major line emissions have been considered.

(3) SPEAC module: This is an interface which connects the module (1), (2) and the dose rate program DRAPKI. The code SPEAC performs the function of cross section mixing, and extracts the activity data from SPAC library based upon the user's selection of the neutron spectrum, cooling time and pulsing scenario.

(4) DRAPKI module: This performs the dose rate calculation using point kernel equations such as Eq. (3) and (4). The code has the capability of calculating the dose rate for both externally shielded and unshielded systems, in addition to the option of choosing different source geometry.

(5) MACT module: This is a post-processor for the DRAPKI module. The code MACT manipulates the data file, making interpolation for graphics and tables.

(6) NOSAM module: This tabulates the normalized activity for a given material at various cooling time. Such tabulations single out the most important contributor to the dose rate at a given time. This information is essential to the understanding of the activation characteristics of a material.

III. ASSUMPTIONS AND VALIDITY

The assumptions involved in deriving the sample material dose rates were as follows:

(1) The neutron flux spectrum was unperturbed in the presence of the sample.

(2) The neutron flux was uniform in the sample.

(3) Photoelectric cross section discontinuities due to the K and L electron shells were ignored.

(4) Only major gamma-ray line emissions such as those reported in Ref. 4 were included.

(5) Instead of matching cross section throughout the entire energy range to find out the effective atomic number, Z, as suggested by Goldstein in order to interpolate the build up factor (Ref. 6), the Compton scattering effective Z was calculated for a material. The dose build-up factor for a point mono-energetic source in an infinite medium with atomic number Z closest to the effective Z for that material then was used. No interpolation was performed.

(6) The samples were in total isolation, that is no external scattering, shielding and build-up were considered.

For small, thin sample, assumptions (1) and (2) are obviously valid. For thick samples, particularly for high Z materials, the activation deep inside the material contributes only minimally to the surface dose rate. Since the neutron flux near the surface is hardly perturbed, the assumptions should also be applicable to thick high Z samples. Furthermore, these assumptions are conservative, resulting in an overestimation for threshold reactions because the neutron attenuation was ignored.

The omission of cross section discontinuity due to the K and L shell photoelectric phenomenon would only effect isotopes decaying with gamma-ray energy in the neighborhood of those discontinuities in the point kernel calculations. Such shell quantum effects are important only for high Z material at low energies. For example, the K shell photoelectric edge occures at 88 keV for Pb and at 20 keV for Mo. Using smooth interpolation of the attenuation coefficient across the discontinuity results in overestimation of the attenuation just above the discontinuity and an underestimation just below the discontinuity. Since the total cross section at lower energies tends to be higher, and the number of gamma-rays which have energies in the neighborhood of the shell edge is small, the omission of the photoelectric edge should not result in any significant error in the point kernel calculations.

The dose build-up factor used in the calculation was based on the Taylor-form (exponential sum) fitting (Ref. 7) of the Goldstein-Wilkins data (Ref. 8). The build-up factors, according to the authors, are believed to be good to ±5% on the average and interpolation in E, Z or penetration should no more than double these errors. The Taylor-form fitting resulted in a maximum deviation for Goldstein-Wilkins data, on the average, of ±10%. The maximum error of using the closest effective Z rather than the interpolation in Z is estimate to be about 20%.

IV. ACTIVATION DOSE RATE DATA FOR STANDARD SAMPLE MATERIALS

The dose rates as a function of cooling time for standard sample materials are illustrated in Fig. 1 to Fig. 24. The smooth curves were obtained by using piecewise Hermite polynomials to interpolate the discrete values calculated at cooling times of ~ 0 hour, 1 hour, 4 hours, 1 day, 2 days, 1 week, 2 weeks, 2 months, 6 months, 1 year, 2 years and 5 years. The materials have been classified according to their functional use:

(1) Structural materials: SS-304, SS-316, A-286, Nitronic-33, Ti-6Al-4V, Inconel 625, Al-6061, Carbon Steel,

(2) Potential materials: SS-304,SS-316, PCA, Modified 9Cr-1Mo, LRO-15, Ti6242s, Vanstar-7, 94Nb-5Mo-1Zr,

(3) Joints and welds: Al,SS-304, Hi-Velcro, Nimonic-90,

(4) Brazes, solders and surface treatment: Yellow brass, Cu-Sn, Cu-Ag, Wiping solder, Soft solder,

(5) Inside vessel materials: SS-304,A-286, Constantan, Inconel X750, TiC, W and Mo,

(6) Diagnostic window materials: Quartz, MgF2, ZnSe, AgCl,

(7) Coils and breaks: Cu, alumina.

The dose rates from SS-304 have been included in every illustration for comparison.

The nominal material composition and density are listed in Table 1. It may be observed that the structural materials studied here include typical stainless steel (SS-304, SS-316), high temperature Cr-Fe-Ni alloy (A-286), high Mn content alloy (Nitronic-33), Ni-based alloy (Inconel, Nimonic), Fe-based alloy (carbon steel, modified 9Cr-1Mo), Ti-based alloy (Ti-6242s and Ti-6Al-4V), vanadium base alloy (Vanstar-7), Niobium based alloy (94Nb-5Mo-1Zr), and aluminium based alloy (Al and Al-6061). The material LRO-15 is a path D candidate in the U.S. Fusion Materials Program (Ref. 9). Even though the high Co content makes the long term residual radioactivity undesirable, the LRO-15 is of interest in this study because of the relatively even distribution of the Fe, Ni, Co and V.

The details of the relative importance of isotope activities for SS-304 are given in Table 2. The important isotopes contributing to the dose rate from other materials are shown in Table 3. While many neutron interactions have been considered in the calculations, the following reactions are responsible for almost all the activities:

$$
\begin{aligned}
&(1)\quad {}^{A}_{Z}N\ (n,\ 2n)\ {}^{A-1}_{Z}N \\
&(2)\quad {}^{A}_{Z}N\ (n,\ \gamma)\ {}^{A+1}_{Z}N \\
&(3)\quad {}^{A}_{Z}N\ (n,\ p)\ {}^{A}_{Z-1}N \\
&(4)\quad {}^{A}_{Z}N\ (n,\ \alpha)\ {}^{A-3}_{Z-2}N\ .
\end{aligned}
\tag{14}
$$

The reaction cross sections weighted by the typical spectrum may be found in the tables of Ref. 1.

The plots presented here give a direct comparison of the activation properties of various materials. Looking at Fig. 1 for the structural materials used for the TFTR with S2 neutron spectrum for instance, Ti-6Al-4V releases the highest dose rate after about 2 days of cooling due to the Na-24 induced by the Al-27(n,α)Na-24 reaction. A few hours after shutdown, on the other hand, it is Mn-56 induced by the Fe-56(n,p)Mn-56 and the Mn-55(n,γ)Mn-56 reactions dominating the dose field so that Nitronic-33 which has the highest combinations of Fe and Mn gives off the highest dose rate. Looking at Table 1 and 2, one can see that Co-58 induced by the Ni-58(n,p)Co-58 reaction is the most important isotope for cooling time greater than 2 weeks and less than about 6 months, consequently the relative magnitude of the dose rate is porportional to the Ni contents of the materials with some contaminations from the Cr-51 isotope. Inconel 625, which is a Ni-based alloy undoubtly gives the highest dose rate during this period of time. After about a year of cooling, Mn-54 induced by the Mn-55(n,2n)Mn-54 and the Fe-54(n,p)Mn-54 reactions becomes dominant, thus again the dose rate from Nitronic-33 is the highest. Co-60 from the Ni-60(n,p)Co-60 reaction then becomes dominant for more than 2 years of cooling so that the higher the Ni content is in a material, the higher the dose rate which can be expected. Notice that both the Ni-58(n,p) Co-58 and the Fe-54(n,p)Mn-54 reactions have thresholds less than the DD neutron energy. Further, the Mn-55(n,γ)Mn-56 reaction has a fairly high cross section in the thermal region (13.6 barns). Two conclusions can be drawn. The first one is that for DD induced activations, the important isotopes contributing to the dose rate for

Cr-Fe-Ni alloys, are the same as those in the DT neutron environment for cooling time greater than a few minutes and less than 2 years. The second is that the Mn content, though small in most of the Cr-Fe-Ni alloys, is important in terms of the activation a few hours after shutdown for a soft neutron spectrum. Taking SS-304 activation one hour after DT operation for example, the 2% Mn contributes about 3.5% of the total dose rate for the S2 spectrum. For the S4 spectrum, however, the Mn contribution increases to about 70%, and for the S6 spectrum the contribution is about 98%.

The magnitude of the dose rate for the standard sample is obtained by first choosing the neutron spectrum closest to the one listed in Section II, and then multiplying the data corresponding to that spectrum by the total neutron flux level. For example, the neutron flux level is expected to be $1.0 \times 10^{13} n/cm^2$-sec near the vaccum vessel during the TFTR DT pulsing, thus the surface dose rate of a 0.0127-m-radius SS-304 ball will be cooled down to 1 mrem/hr after about 3 years. For materials similiar in composition and density but different in other details, the dose rate may be scaled directly from those shown in the figures.

It should be pointed out that in some cases, the small amount of additives could substantially alter the profile of activation for a material. The molybdenum in SS-316, for instance, shows importance after one day of cooling (Mo-99 and its daughter Tc-99m), especially for the DD neutron induced activation. Perhaps the best example is the activation of Al-6061. After a few minutes of cooling, the dose rate from Al-6061 exposed to DD neutrons is predominantly due to the small amount of Cu and Cr. Similarly, after two weeks of cooling, the activation of Al-6061 induced by the DT neutrons is again determined by those impurities.

Materials containing silver give rise to much higher dose rate compared to SS-304 for cooling time greater than 2 days and less than 2 years. Silver is known to be a good neutron absorber; the Ag-109 isotope has a neutron capture resonance cross section as high as 5000 barns at about

5 eV. The capture product could either be Ag-110 or Ag-110m with half-lives of 25 seconds and 252 days respectively. Since a 50-50 partition has been assigned to the reaction products in the calculation, the error in the Ag activation dose rate is dependent on this assignment. Local hot spots may be expected near Ag containing materials such as the Cu-Ag brazing. Nevertheless, the amount of silver is expected to be small and the locations will be scattered, so that the global field is not expected to alter significantly.

V. EFFECT OF PULSING SCENARIO, SAMPLE SIZE AND OBSERVATION DISTANCE

(a) Pulsing modification factor, fp

The relative pulsing factor, fp, has been defined in Eq. (11). Clearly, fp is a function of cooling time and location where the sample was irradiated. Stating this another way, fp depends upon the half-lives of the isotopes contributing to the dose rate. The fp curves for a selected set of sample materials are shown in Figs. 25 to 32. The fp factors for materials not shown in these figures may be estimated by comparing the important isotopes contributing to the dose rate with those of a material for which the fp has been calculated. Alternatively, fp may be computed according to Eqs. (9) and (6) of Ref. 1, or by examining the irradiation history time function shown as Fig. 4 in Ref. 1.

Since the longest pulsing period considered here is only on the order of 10 hours, for cooling time longer than about 2 weeks such that the isotopes with half-lives much greater than 10 hours dominate the activity, the dose rate is proportional to the number of neutrons produced in a sequence of operation.

(b) Sample size modification factor, fs

The factor fs which has been defined in Eq. (12) is a measure of the dose rate of a material relative to that of a 0.0127-m-radius spherical sample. For a given material, fs depends upon the decay gamma-ray energy of the isotopes important in their contribution to the dose rate, and on the pulsing history. Such dependencies

in general are within ±20% for all the pulsing scenarios, cooling times and the neutron spectral shapes considered in this study, so that scaling according to the density of the material is usually adequate. Figure 33 shows the fs curves as a function of sample characteristic size for Al, Ti-6Al-4V, SS-304 and W with densities of 2.7, 4.4, 8.0 and 19.2 x 10^3 kg/m**3, respectively. The data were derived based on the neutron spectrum S2, and 100 consecutive pulses, after one hour of cooling. Note that the slab data have been normalized to those of the 0.0127-m-radius spheres. The approximate curves for fs as a function of material density are given in Figs. 34 and 35 for spherical and slab objects.

For small samples with low density, fs is approximately a linear function of the dimension. The value of fs levels off beyond a critical thickness of the sample. The higher the density, the smaller the size required to attain saturation and the lower the saturation activity will be when compared to the standard sample. The dose rate due to a 0.254-m-radius aluminum sphere is about a factor of 10 higher than that of a 0.0127-m-radius Al sphere, whereas the ratio for steel is about 3 and for tungstun about 1. For densities greater than 5 x 10^3 kg/m**3, the dose rate saturates for spheres with radii greater than 0.12 m.

It is interesting to compare the relative dose rate due to a 0.0127-m-radius sphere and a 0.0254-m-thick slab. In both cases, the total characteristic thickness of the sample is 0.0254 m. The slab to sphere dose rate ratio is about 2.8 for Al and about 2 and 1 for steel and tungstun respectively. Thus even though the slab is infinite in the vertical extension, the exponential nature of the attentuation and the 1/r**2 dependence of the flux result in the surface dose rate from the slab only a factor of three higher than the surface dose rate from the sphere, for the lightest material of comparable thickness considered here.

(c) *Observation distance modification factor, fd*

Looking at Eq. (13), fd depends on the energies of the decay gamma-rays, the pulsing scenario and the size of the object for a given sample. It has been found that fd is a strong function of the size of the sample and depends very weakly on the other factors, including the density of the materials. Indeed, far enough away from any finite sized object, the dose rate would be proportional to 1/r**2 where the proportionality depends upon the size of the object. The fd curves for Al, Ti-6Al-4V, SS-304, and W are illustrated in Fig. 36 for observation distance from 0.01m to about 10 meters. The data were again based on the S2 neutron spectrum, 100 pulses DT operational scenario and one hour of cooling. Notice that for infinite slab objects, the dose rate is constant throughout the space outside the object itself.

VI. DATA UTILIZATION AND SAMPLE PROBLEMS

For materials similiar in composition and density, direct scaling of the dose rates may be applied. If at a given cooling time, more than one isotope contributes to the dose rate and the isotopes could be produced by more than one reactions, the following example illustrates how the estimation should be made.

Fxample 1: Given the material composition in Table 1 and relative activity for SS-304 in Table 2, find the activity ratio of Mn-54 to Co-58 for Nimonic-90 at the vaccum vessel location after 100 DT pulses.

Define:

C_{304} = activity ratio of ^{54}Mn to ^{58}Co for SS-304.
C_{90} = activity ratio of ^{54}Mn to ^{58}Co for Nimonic-90.
M_i = atomic number of element i.
A(k) = activity of isotope k.
α_i, m = weight perent of element i in material m.
β_j, i = abundance of isotope j in element i.
ϕ = total neutron flux.

R_k = rate of production for isotope k.

$\sigma_{j,k}$ = effective production cross section of isotope k due to neutron interaction with j.

τ_k = irradiation history function for isotope k.

W_k = cooling time function for isotope k.

ρ_m = density of material m.

N_o = Avogadro's number.

From Table 1, the compositions of SS-304 and Nimonic 90 are:

i	αi, 304	αi, 90
Mn	0.02	0.005
Fe	0.69	0.01
Ni	0.10	0.563
Co	0.0	0.180

Consider only those reactions listed in Eq. (14), it is seen that ^{54}Mn can be produced by

(a) ^{55}Mn (n, 2n) ^{54}Mn,

(b) ^{54}Fe (n, p) ^{54}Mn,

and the ^{58}Co can be produced by

(c) ^{59}Co (n, 2n) ^{58}Co,

(d) ^{58}Ni (n, p) ^{58}Co.

From Eq. (14) and Eq. (18) of Ref. 1

$$A(k) = R_k \tau_k W_k \qquad (15)$$

where

$$R_k = \sum_i \sum_j N_{i,j} \sigma_{j,k} \phi ,$$

$$= \sum_i \sum_j \frac{N_o \rho_m \alpha_{i,m} \beta_{j,i}}{M_i} \sigma_{j,k} \phi ,$$

$$= N_o \phi \rho_m \left[\sum_i \frac{\alpha_{i,m}}{M_i} \sum_j \beta_{j,i} \sigma_{j,k} \right] ,$$

$$= N_o \phi \rho_m I_{k,m} . \qquad (16)$$

Reading $\sigma_{j,k}$ from Table I.A and III.A of Ref. 1, the following tables can be constructed.

Table (a)

k	i	j	$\sigma_{j,k}$	$\beta_{j,i}$
^{54}Mn	Mn	^{55}Mn	0.202	1.0
^{54}Mn	Fe	^{54}Fe	0.123	0.058
^{58}Co	Ni	^{58}Ni	0.135	0.683
^{58}Co	Co	^{58}Co	0.167	1.0

Table (b)

M	k	$I_{k,m}$
SS-304	^{54}Mn	0.0162
SS-304	^{58}Co	0.0157
Nimonic-90	^{54}Mn	0.0020
Nimonic-90	^{58}Co	0.1394

Since

$$A_m = \frac{A(k_1)}{A(k_2)} = \frac{I_{k1,m}}{I_{k2,m}} \frac{\tau_{k1}}{\tau_{k2}} \frac{W_{k1}}{W_{k2}} \qquad (17)$$

let $k1 = {}^{54}Mn$

$k2 = {}^{58}Co$,

and

$$\Gamma = \frac{\tau_{k1}\ W_{k1}}{\tau_{k2}\ W_{k2}} \tag{18}$$

then

$$A_{304} = \frac{0.0162}{0.0157}\ \Gamma = 1.032\ \Gamma \tag{19}$$

$$A_{90} = \frac{0.0020}{0.1394}\ \Gamma = 0.014\ \Gamma \tag{20}$$

or

$$A_{90} = 0.014\ A_{304}\ . \tag{21}$$

Reading from Table 2 for A_{304}, one obtains

t_w	A_{304}	A_{90}(calc.)	A_{90} (actual)
2 months	0.367	0.005	0.005
6 months	0.912	0.013	0.013
1 year	3.686	0.052	0.051

Example 2: Estimate the dose rate from a standard Nimonic-90 sample after 6 months of cooling given the dose rate of 2.1×10^{-12} mrem/hr for a SS-304 standard sample. Assume that the samples have been irradiated on the vessel during the DT operation.

Consider the following isotopes, letting

$$k1 = {}^{54}Mn$$

$$k2 = {}^{58}Co$$

$$k3 = {}^{60}Co$$

Let ε_k be the relative importance for a given isotope in its contribution to the dose rate (~ proportional to the total gamma-ray energy intensity), and let f_k be the fractional dose rate due to isotope k. From Table 2 for SS-304,

k	ε_k	f_k
^{54}Mn	1.0	0.47
^{58}Co	1.0	0.50
^{60}Co	2.8	0.03

Let D_m be the dose rate from material m and $A_m(k)$ be the activity of isotope k in material m at cooling time t_w, then

$$D_{90} = D_{304} \sum_k f_k \frac{A_{90}(k)}{A_{304}(k)}$$

$$= D_{304} \frac{\rho_{90}}{\rho_{304}} \sum_k f_k \frac{I_{k,90}}{I_{k,304}} \qquad (22)$$

where ρ_m and $I_{k,m}$ have the same definitions as in Example 1.

Compute $I_{k,m}$ for ^{60}Co in a manner similar to those in Example 1, one obtains

$$I_{k,90} = 0.0493$$

and $I_{k,304} = 0.0017.$

It follows that,

$$D_{90} = D_{304} \frac{\rho_{90}}{\rho_{304}} \left[0.47 \ \frac{0.0020}{0.0162} + 0.50 \ \frac{0.1394}{0.0157} + 0.03 \ \frac{0.0493}{0.0017}\right] . \qquad (23)$$

Since

$$\rho_{90} = 8.18 \times 10^{-3} \text{ kg/m}^3,$$

$$\rho_{304} = 8.03 \times 10^{-3} \text{ kg/m}^3,$$

and $D_{304} = 2.1 \times 10^{-12}$ mrem/hr

therefore,

$$D_{90} = 1.15 \times 10^{-11} \text{ mrem/hr.}$$

Reading from Fig. 11, the computer calculation gives a value of 1.3×10^{-11} mrem/hr. Thus the estimate here has an error of only 10%. The data presented in this report are for a single pulsing sequence (e.g., a sequence of 100 consecutive pulses). For the case of multiple pulsing sequences the results are additive so long as the proper decay time is taken into account. That is

$$D(t) = \sum_{\ell} D_{\ell} \left(t - t_{\ell}\right) \tag{24}$$

where

$D(t)$ = total dose rate at time t,

$D_{\ell}(t)$ = dose rate due to the ℓ^{th} pulsing sequence,

and

t_{ℓ} = the time where the ℓ^{th} pulsing sequence terminated.

The following example shows how this can be done.

Example 3: Assume 50 DD pulses are made starting the first day of the first week, 100 DD pulses are made starting the first day of the second week and 10 DT pulses are made starting the first day of the third week. Assume further that no DT burn takes place during a DD pulse and that the neutron flux levels on the vessel are 1.0×10^{11} and 1.0×10^{13} for DD and DT operation respectively. Calculate the dose rate on the surface of a 0.0127-m-radius SS-304 spherical nut two weeks after the last DT pulse.

Let t_{ℓ} be the cooling time after the ℓ^{th} pulsing

then

t_1 = 27.86 days

t_2 = 20.60 days

t_3 = 14.0 days.

Reading from Figs. 1 and 8 for the dose rate values and from Figs. 25 and 26 for the values of fp, then based on Eqs. (10) and (24), one obtains

$$D = D_1\,(27.86d) + D_2\,(20.69d) + D_3\,(14\ d)$$

$$= (1.5 \times 10^{12} \times 0.5 + 1.6 \times 10^{-12} \times 1.0) \times 10^{11}$$

$$+ 7.7 \times 10^{-12} \times 0.1 \times 10^{13} \qquad (25)$$

$$= 8\ \text{mrem/hr}.$$

ACKNOWLEDGEMENTS

We wish to express our sincere thanks to G.V. Sheffield and J.T. Giarrusso for their constant encouragement and administrative help.

This work was supported by the U.S. DOE Contract No. DE-AC02-76-CHO-3073.

REFERENCES

(1) Long-poe Ku and J.G. Kolibal, "Estimated Neutron Activation Data for TFTR, Part I. The Specific Radioactivities, " PPPL-1847 (1981).

(2) J.J. Taylor et. al, "Applications of Gamma-ray Buildup Data to Shield Design," WAPD RM-217 (1954).

(3) Hironori Ono and Akira Tsuruo, "An Approximate Calculation Method of Flux for Spherical and Cylindrical Sources with a Slab Shield," Journal of Nuclear Science and Technology, 2, (6), 229 (1965).

(4) A. Foderaro, "The Photon Shielding Manual," The Penn State Bookstore (1979).

(5) C.M. Lederer and V. S. Shirley ed., "Table of Isotopes," 7th Edition, John Wiley and Sons, Inc. (1978).

(6) H. Goldstein, "Fundamental Aspects of Reactor Shielding," Addison-Wesley Publishing Company, Inc. (Reprinted by Johnson Reprint Corporation, 1971).

(7) S. Buscaglione and R. Manzini, "Buildup Factor: Coefficients of the J.J. Taylor Equation," ORNL-tr-80 (1965).

(8) H. Goldstein and J.E. Wilkins, Jr., "Calculation of the Penetration of Gamma Rays," USAEC report NYO-3075 (1954)

(9) R.E. Gold et. al., "Materials Technology for Fusion: Current Status and Future Requirements," Nuclear Technology/Fusion, Vol. 1, No. 2. 169 (1981).

Definition of Weighting Flux Spectrum

S2: The spectrum at the TFTR vaccum vessel due to DT neutrons;

S3: the spectrum at the TFTR test cell center, without igloo shield, due to DT neutrons;

S4: the spectrum for DT neutrons attenuated by a 0.66-m Limestone concrete shield with a borated concrete reflector behind the shield;

S5: the same as S4, except that the shield thickness has been increased to 0.86 m;

S6: the spectrum for DT neutrons attenuated by a 1.83 m of Limestone concrete shield with an ordinary concrete reflector behind the shield;

S8: the same as S2, except for DD neutrons;

S9: the same as S3, except for DD neutrons; and,

S10: the same as S6 except for DD neutrons.

FIGURE CAPTIONS

Fig. 1. Dose rate as a function of cooling time, S2 spectrum, 1=Nitronic-33, 2=SS-304, 3=SS-316, 4=A-286, 5=Inconel-625, 6=Ti-6Al-4V.

Fig. 2. Dose rate as a function of cooling time, S2 Spectrum, 1=94Nb-5Mo-1Zr, 2=Vanstar-7, 3=Ti-6242s, 4=LRO-15, 5=PCA, 6=SS-316, 7=SS-3904, 8=9Cr-1Mo.

Fig. 3. Dose rate as a function of cooling time, S3 spectrum, 1=Al-6061, 2=Cu, 3=Carbon Steel, 4=SS-304.

Fig. 4. Dose rate as a function of cooling time, S4 spectrum, 1=Al, 2=Cu, 3=Carbon Steel, 4=SS-304.

Fig. 5. Dose rate as a function of cooling time, S5 spectrum, 1=Al-6061, 2=Carbon Steel, 3=SS-304.

Fig. 6. Dose rate as a function of cooling time, S6 spectrum, 1=Al-6061, 2=Cu, 3=Carbon Steel, 4=SS-304.

Fig. 7. Dose rate as a function of cooling time, S8 spectrum, 1=Ti-6Al-4V, 2=Nitronic-33, 3=SS-304, 4=SS-316, 5=A-286, 6=Inconel-625.

Fig. 8. Dose rate as a function of cooling time, S8 spectrum, 1=Vanstar-7, 2=LRO 5, 3=Ti-6242s, 4=Nb-5Mo-1Zr, 5=9Cr-1Mo, 6=SS-304, 7=SS-316, 8=PCA.

Fig. 9. Dose rate as a function of cooling time, S9 spectrum, 1=Al-6061, 2=Cu, 3=Carbon Steel, 4=SS-304.

Fig. 10. Dose rate as a function of cooling time, S10 Spectrum, 1=Al-6061, 2=Cu, 3=Carbon Steel, 4=SS-304.

Fig. 11. Dose rate as a function of cooling time, S2 spectrum, 1=Al, 2=SS-304, 3=Hi-Velcro, 4=Nimonic-90.

Fig. 12. Dose rate as a function of cooling time, S8 spectrum, 1=Al, 2=SS-304, 3=Hi-Velcro, 4=Nimonic-90 .

Fig. 13. Dose rate as a function of cooling time, S2 spectrum, 1=Soft solder, 2=Wiping solder, 3=Cu-Sn braze, 4=Yellow brass, 5=SS-304, 6=Cu-Ag braze.

Fig. 14. Dose rate as a function of cooling time, S3 spectrum, 1=Soft solder, 2=Wiping solder, 3=Cu-Sn braze, 4=Yellow brass, 5=SS-304, 6=Cu-Ag braze.

Fig. 15. Dose rate as a function of cooling time, S8 spectrum, 1=Soft solder, 2=Wiping solder, 3=Cu-Sn braze, 4=Yellow brass, 5=SS-304, 6=Cu-Ag braze.

Fig. 16. Dose rate as a function of cooling time, S9 spectrum, 1=Soft solder, 2=Wiping solder, 3=SS-304, 4=Cu-Sn braze, 5=Yellow brass, 6=Cu-Ag braze.

Fig. 17. Dose rate as a function of cooling time, S2 spectrum, 1=SS-304, 2=A-286, 3=Constantan, 4=Inconel-X750.

Fig. 18. Dose rate as a function of cooling time, S2 spectrum, 1=SS-304, 2=W, 3=Mo, 4=TiC.

Fig. 19. Dose rate as a function of cooling time, S8 spectrum, 1=SS-304, 2=A-286, 3=Constantan, 4=Inconel-X750.

Fig. 20. Dose rate as a function of cooling time, S8 spectrum, 1=TiC, 2=SS-304, 3=Mo, 4=W.

Fig. 21. Dose rate as a function of cooling time, S2 spectrum, 1=Quartz, 2=MgF2, 3=ZnSe, 4=SS-304, 5=AgCl.

Fig. 22. Dose rate as a function of cooling time, S8 spectrum, 1=Quartz, 2=MgF2, 3=ZnSe, 4=SS-304, 5=AgCl.

Fig. 23. Dose rate as a function of cooling time, S2 spectrum, 1=Al, 2=Cu, 3=SS-304.

Fig. 24. Dose rate as a function of cooling time, S8 spectrum, 1=Al, 2=Cu, 3=SS-304.

Fig. 25. Relative dose rate as a function of number of pulses. S2 spectrum.

Fig. 26. Relative dose rate as a function of number of pulses, S2 spectrum.

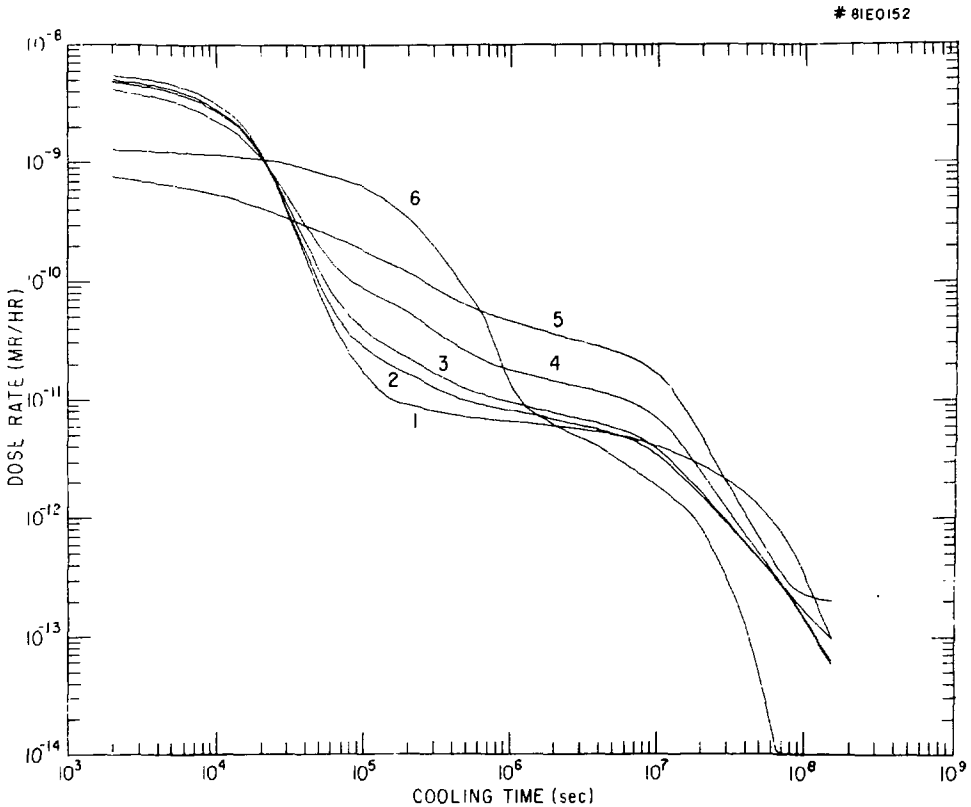

Fig. 1. Dose rate as a function of cooling time, S2 spectrum, 1=Nitronic-33, 2=SS-304, 3=SS-316, 4=A-286, 5=Inconel-625, 6=Ti-6Al-4V.

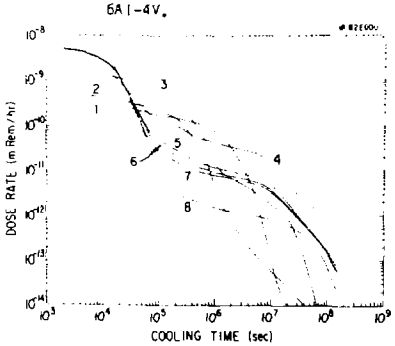

Fig. 2. Dose rate as a function of cooling time, S2 Spectrum, 1=94Nb-5Mo-1Zr, 2=Vanstar-7, 3=Ti-6242s, 4=LRO-15, 5=PCA, 6=SS-316, 7=SS-3904, 8=9Cr-1Mo.

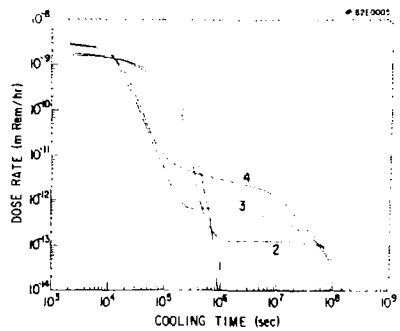

Fig. 3. Dose rate as a function of cooling time, S3 spectrum, 1=Al-6061, 2=Cu, 3=Carbon Steel, 4=SS-304.

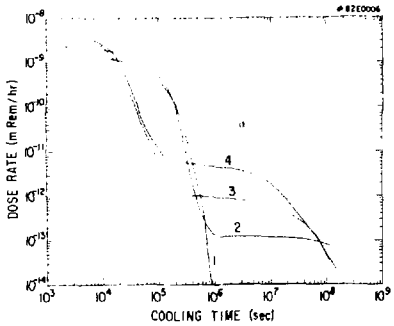

Fig. 4. Dose rate as a function of cooling time, S4 spectrum, 1=Al, 2=Cu, 3=Carbon Steel, 4=SS-304.

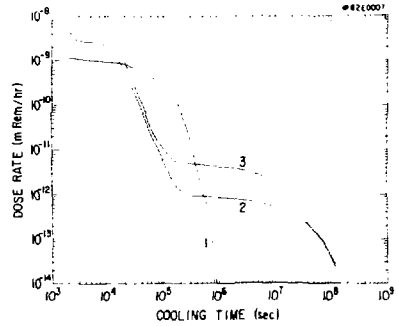

Fig. 5. Dose rate as a function of cooling time, S5 spectrum, 1=Al-6061, 2=Carbon Steel, 3=SS-304.

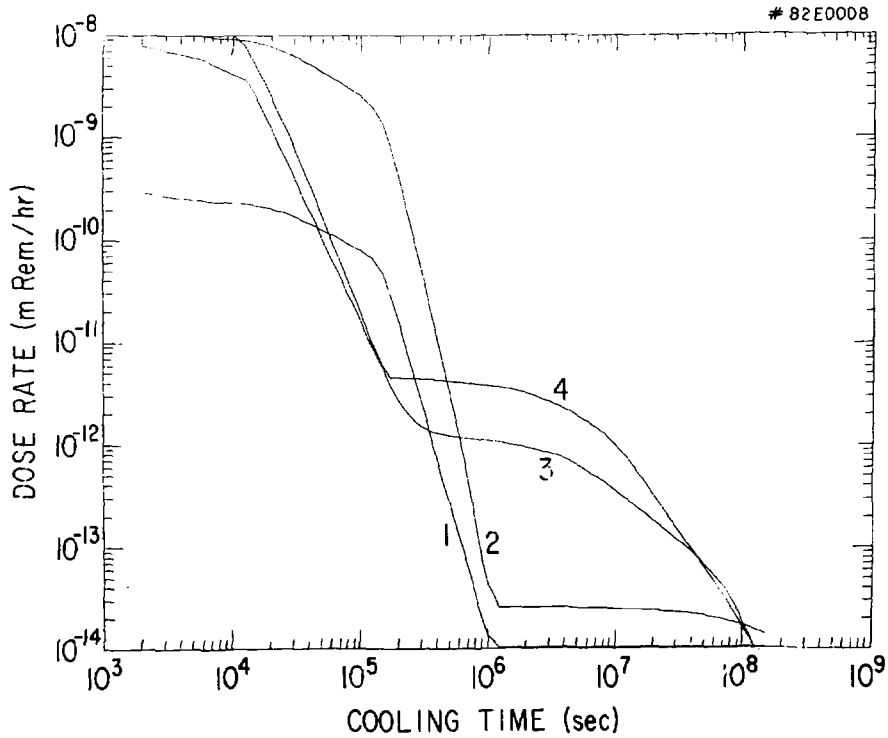

Fig. 6. Dose rate as a function of cooling time, S6 spectrum, 1=Al-6061, 2=Cu, 3=Carbon Steel, 4=SS-304.

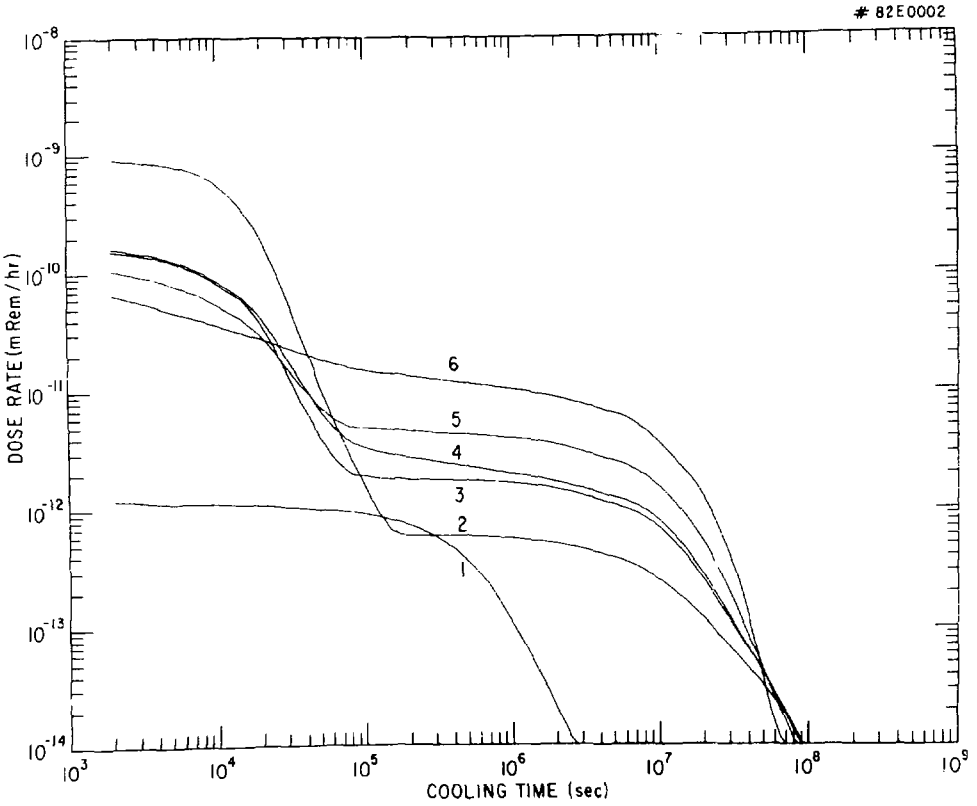

Fig. 7. Dose rate as a function of cooling time, S8 spectrum, 1=Ti-6Al-4V, 2=Nitronic-33, 3=SS-304, 4=SS-316, 5=A-286, 6=Inconel-625.

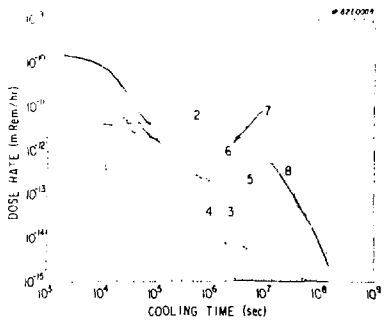

Fig. 8. Dose rate as a function of cooling time, S8 spectrum, 1=Vanstar-7, 2=LRO-15, 3=Ti-6242s, 4=Nb-9Mo-1Zr, 5=9Cr-1Mo, 6=SS-304, 7=SS-316, 8=PCA.

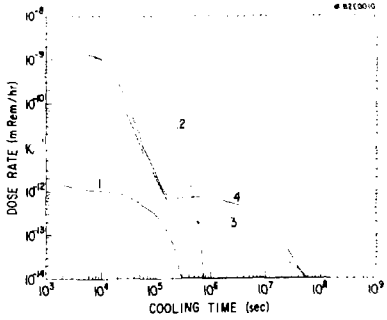

Fig. 9. Dose rate as a function of cooling time, S9 spectrum, 1=Al-6061, 2=Cu, 3=Carbon Steel, 4=SS-304.

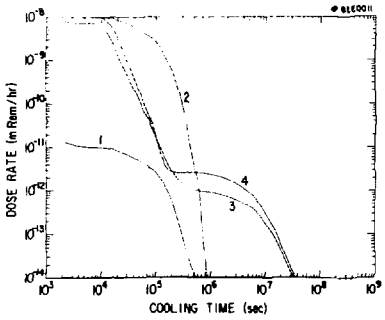

Fig. 10. Dose rate as a function of cooling time, S10 Spectrum, 1=Al-6061, 2=Cu, 3=Carbon Steel, 4=SS-304.

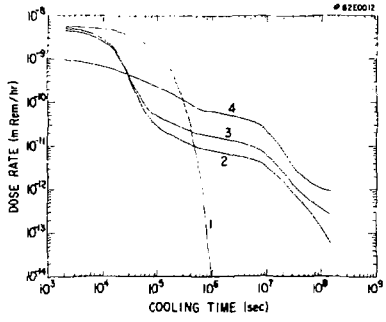

Fig. 11. Dose rate as a function of cooling time, S2 spectrum, 1=Al, 2=SS-304, 3=Hi-Velcro, 4=Nimonic-90.

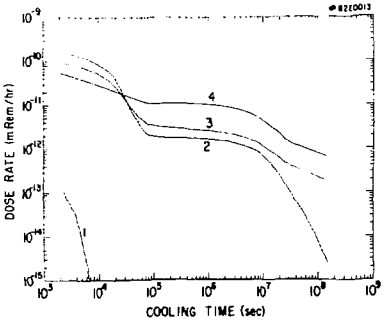

Fig. 12. Dose rate as a function of cooling time, S8 spectrum, 1=Al, 2=SS-304, 3=Hi-Velcro, 4=Nimonic-90 .

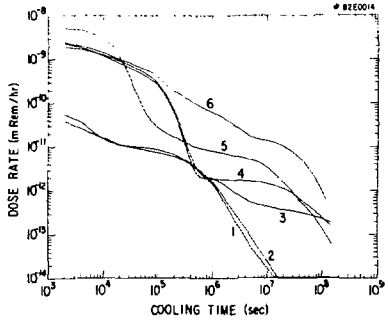

Fig. 13. Dose rate as a function of cooling time, S2 spectrum, 1=Soft solder, 2=Wiping solder, 3=Cu-Sn braze, 4=Yellow brass, 5=SS-304, 6=Cu-Ag braze.

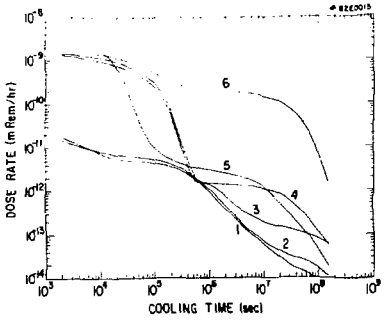

Fig. 14. Dose rate as a function of cooling time, S3 spectrum, 1=Soft solder, 2=Wiping solder, 3=Cu-Sn braze, 4=Yellow brass, 5=SS-304, 6=Cu-Ag braze.

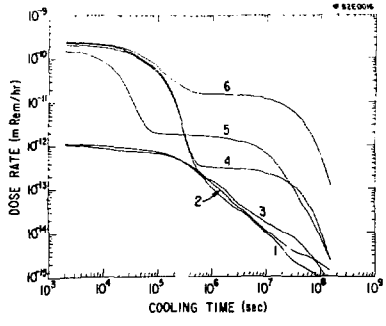

Fig. 15. Dose rate as a function of cooling time, S8 spectrum, 1=Soft solder, 2=Wiping solder, 3=Cu-Sn braze, 4=Yellow brass, 5=SS-304, 6=Cu-Ag braze.

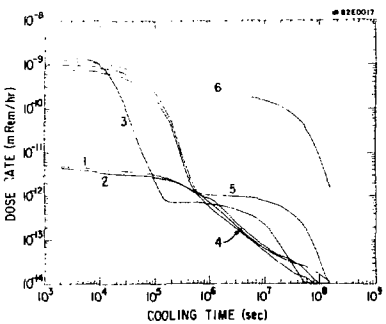

Fig. 16. Dose rate as a function of cooling time, S9 spectrum, 1=Soft solder, 2=Wiping solder, 3=SS-304, 4=Cu-Sn braze, 5=Yellow brass, 6=Cu-Ag braze.

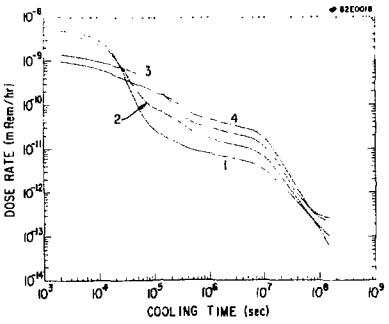

Fig. 17. Dose rate as a function of cooling time, S2 spectrum, 1=SS-304, 2=A-286, 3=Constantan, 4=Inconel-X750.

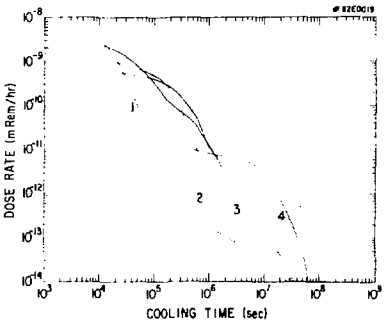

Fig. 18. Dose rate as a function of cooling time, S2 spectrum, 1=SS-304, 2=W, 3=Mo, 4=TIC.

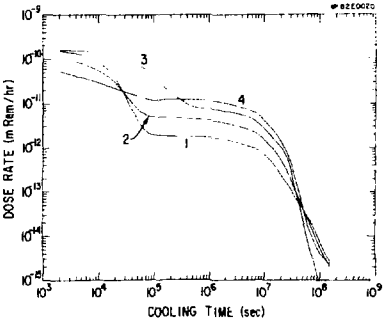

Fig. 19. Dose rate as a function of cooling time, S8 spectrum, 1=SS-304, 2=A-286, 3=Constantan, 4=Inconel-X750.

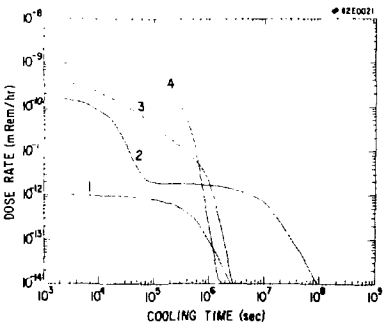

Fig. 20. Dose rate as a function of cooling time, S8 spectrum, 1=TIC, 2=SS-304, 3=Mo, 4=W.

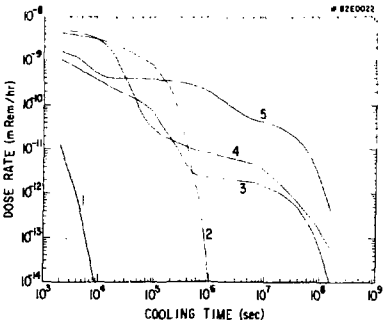

Fig. 21. Dose rate as a function of cooling time, S2 spectrum, 1=Quartz, 2=MgF2, 3=ZnSe, 4=SS-304, 5=AgCl.

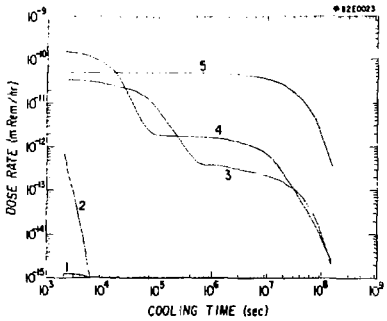

Fig. 22. Dose rate as a function of cooling time, S8 spectrum, 1=Quartz, 2=MgF2, 3=ZnSe, 4=SS-304, 5=AgCl.

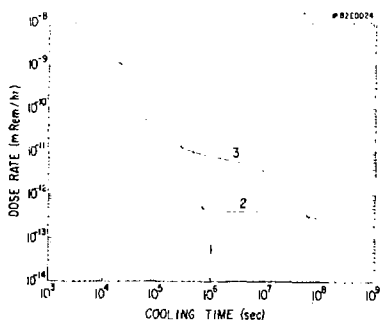

Fig. 23. Dose rate as a function of cooling time, S2 spectrum, 1=Al, 2=Cu, 3=SS-304.

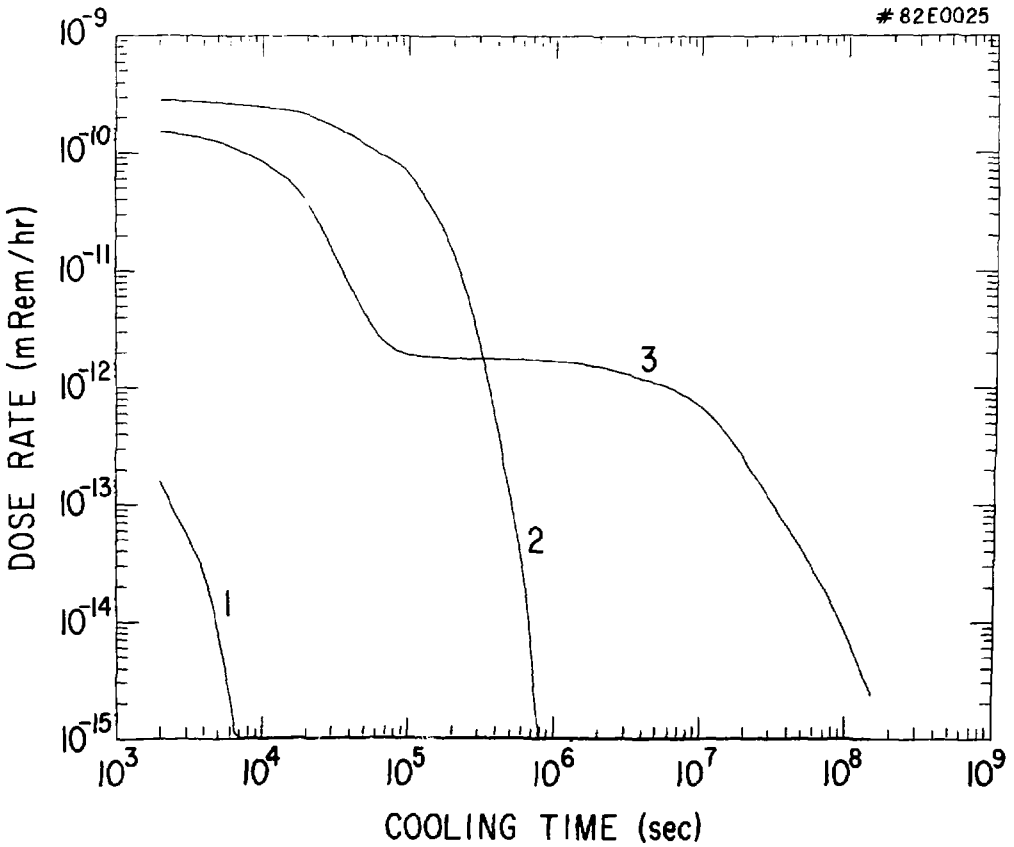

Fig. 24. Dose rate as a function of cooling time, S8 spectrum, 1=Al, 2=Cu, 3=SS-304.

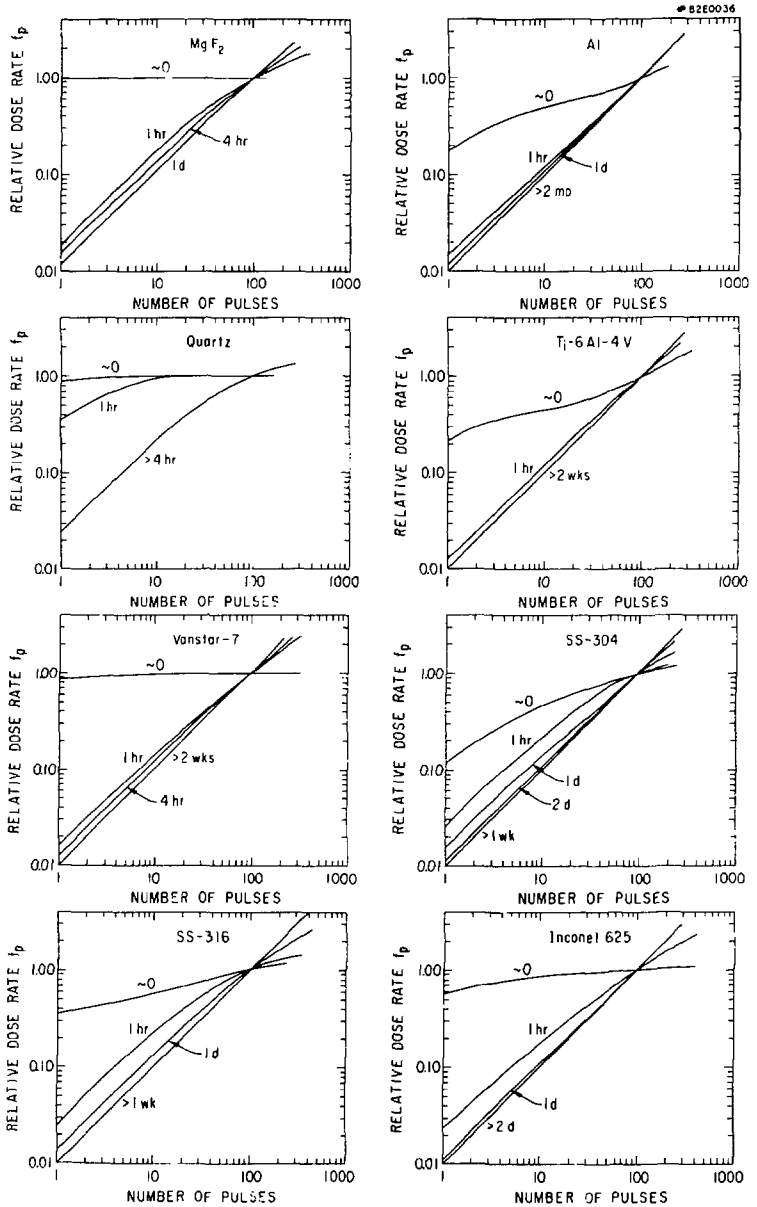

Fig. 25. Relative dose rate as a function of number of pulses, S2 spectrum.

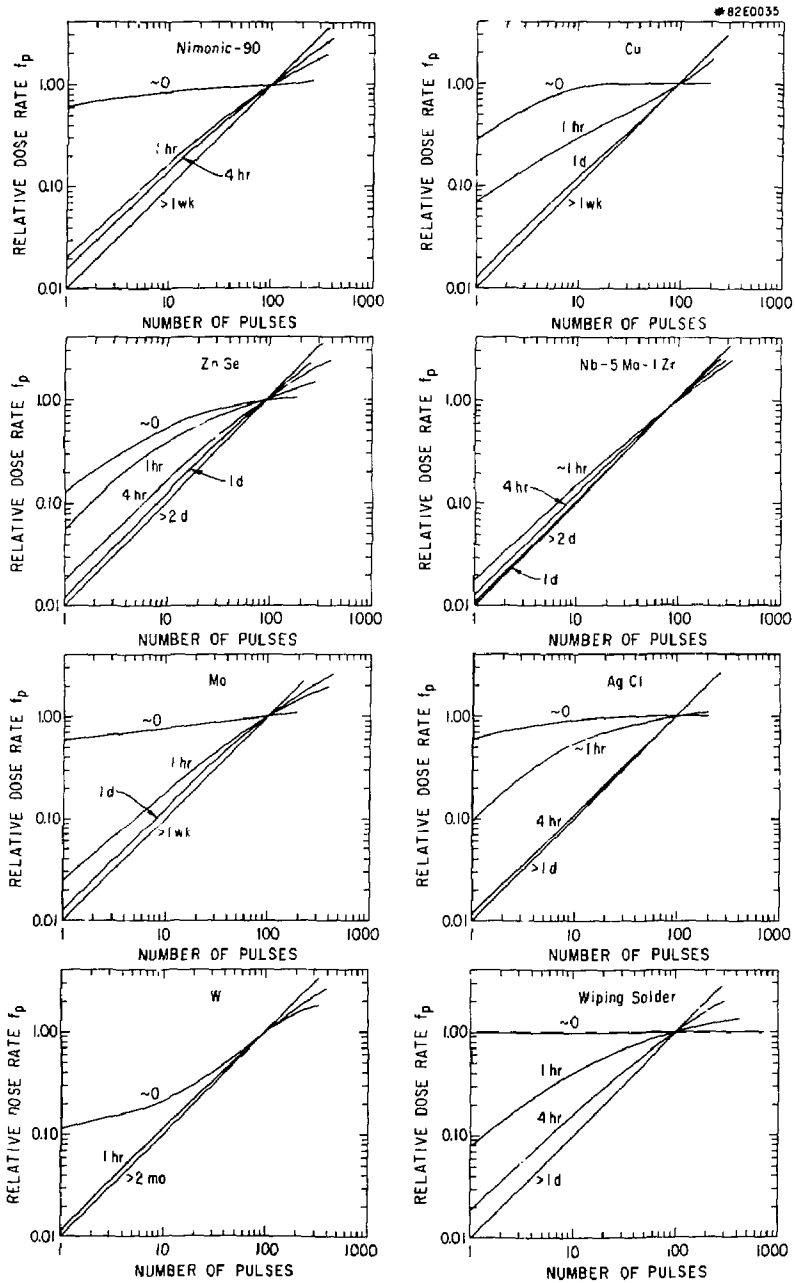

Fig. 26. Relative dose rate as a function of number of pulses, S2 spectrum.

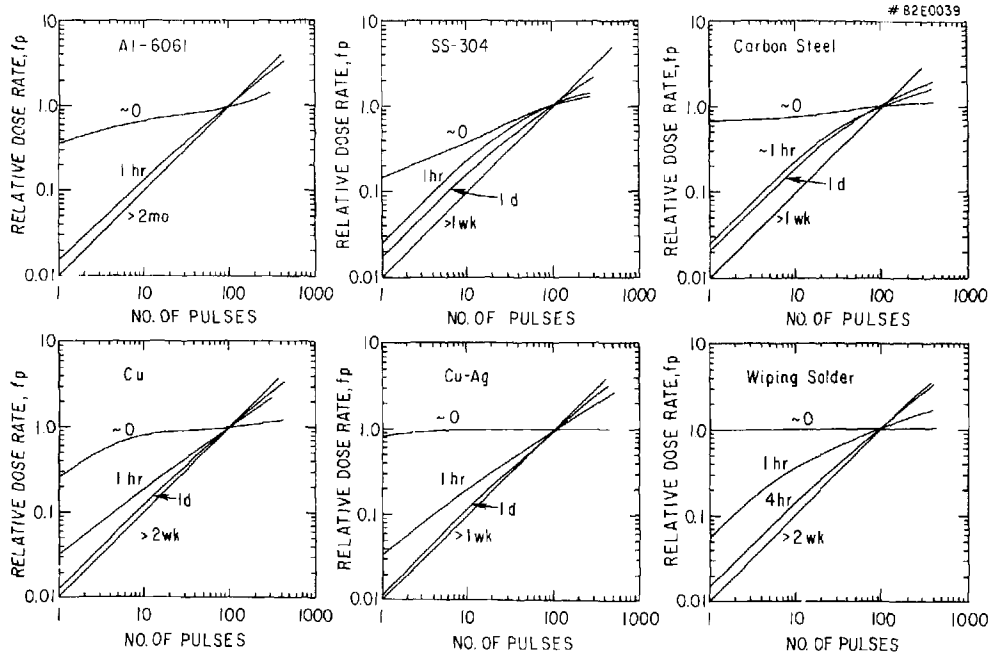

Fig. 27. Relative dose rate as a function of number of pulses, 53 spectrum.

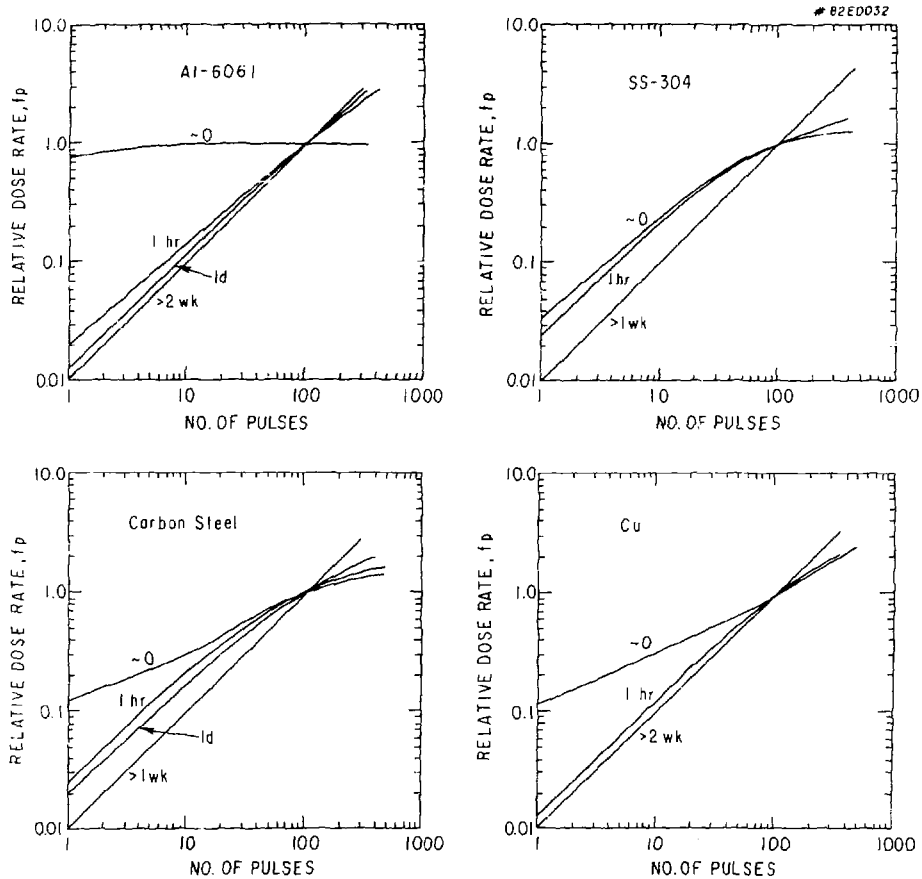

Fig. 23. Relative dose rate as a function of number of pulses, S6 spectrum.

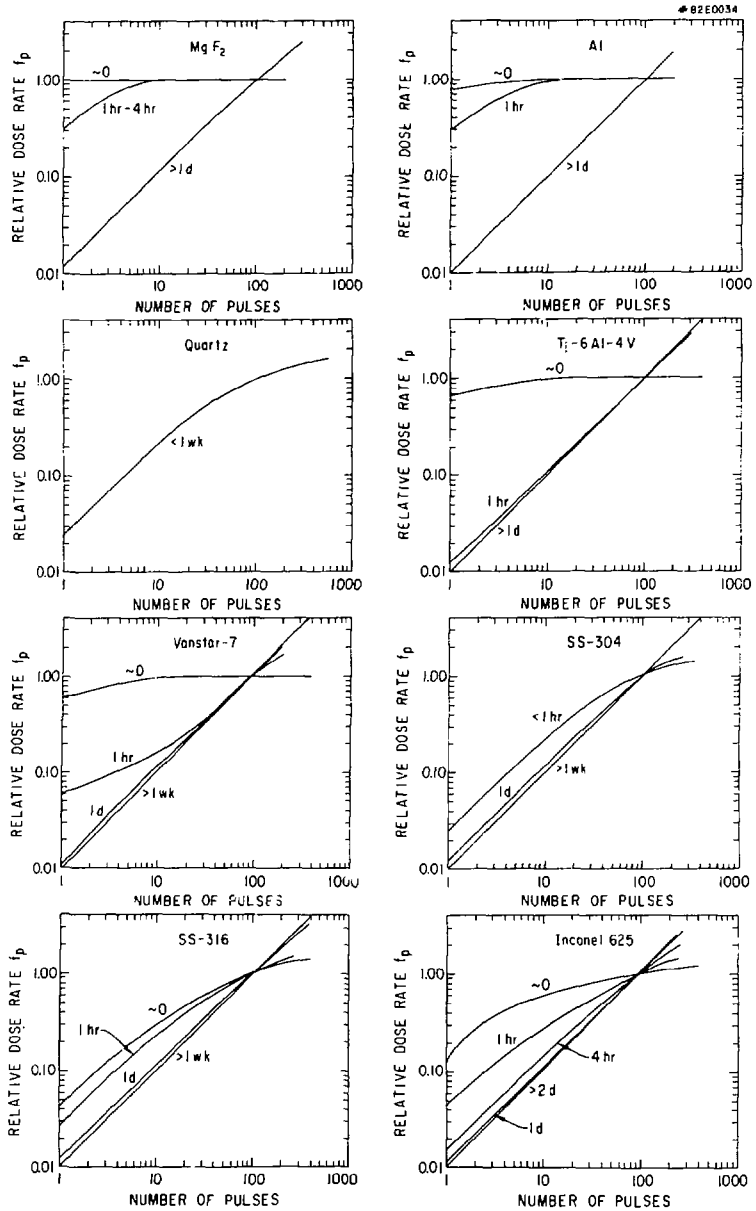

Fig. 29. Relative dose rate as a function of number of pulses, S8 spectrum.

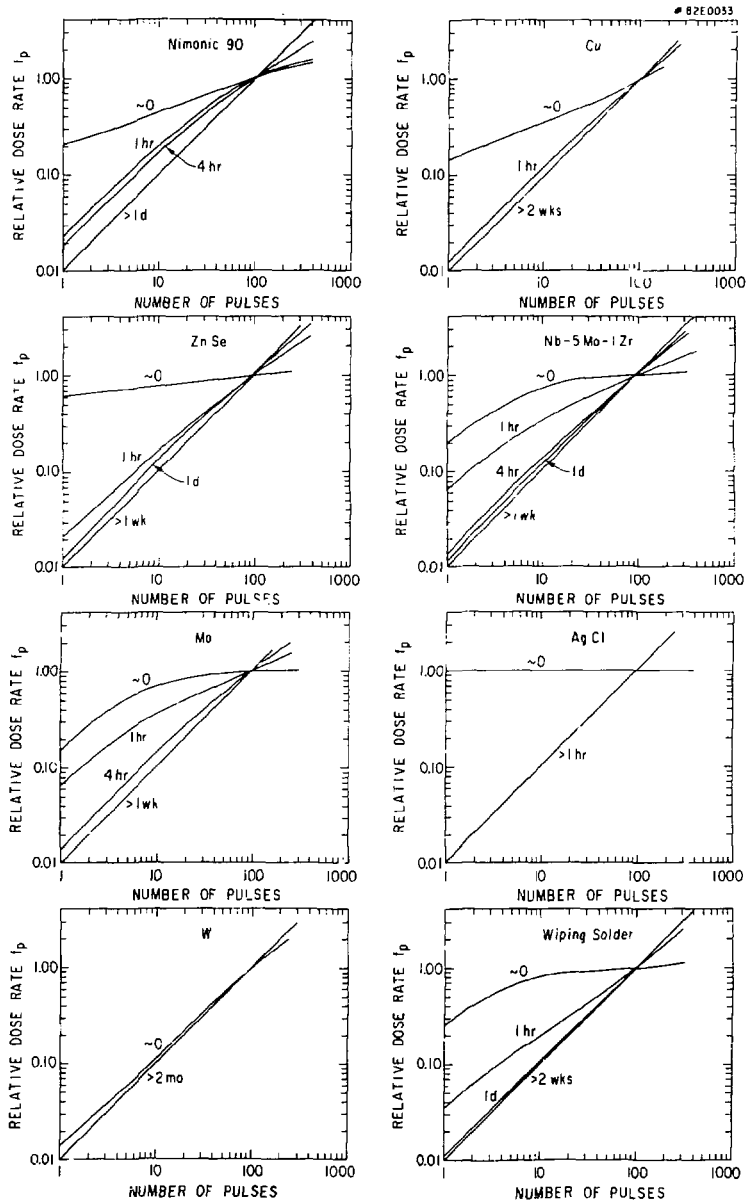

Fig. 30. Relative dose rate as a function of number of pulses, S8 spectrum.

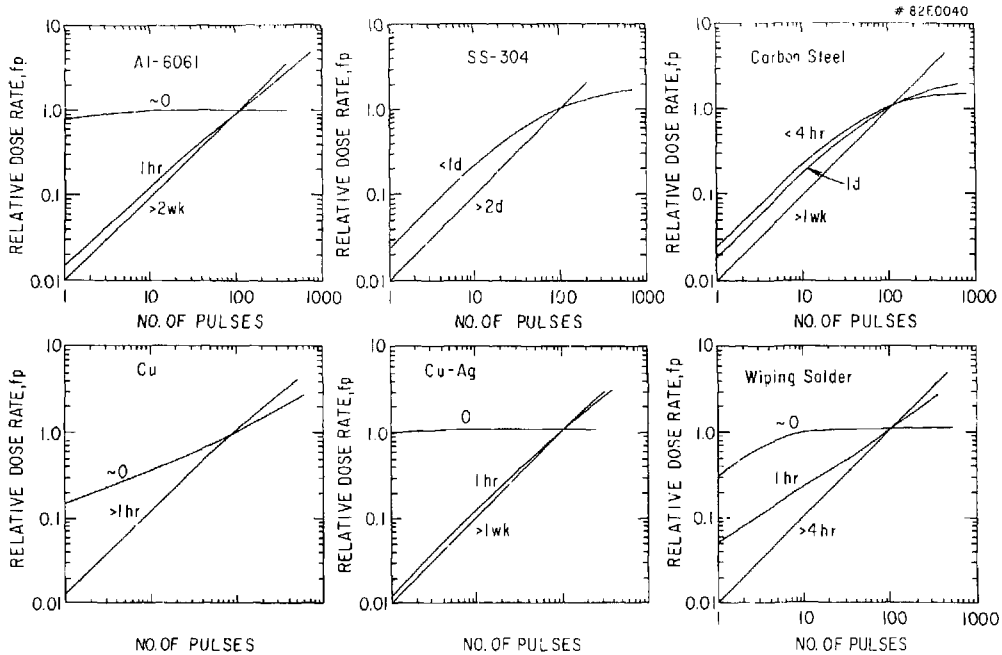

Fig. 31. Relative dose rate as a function of number of pulses, S9 spectrum.

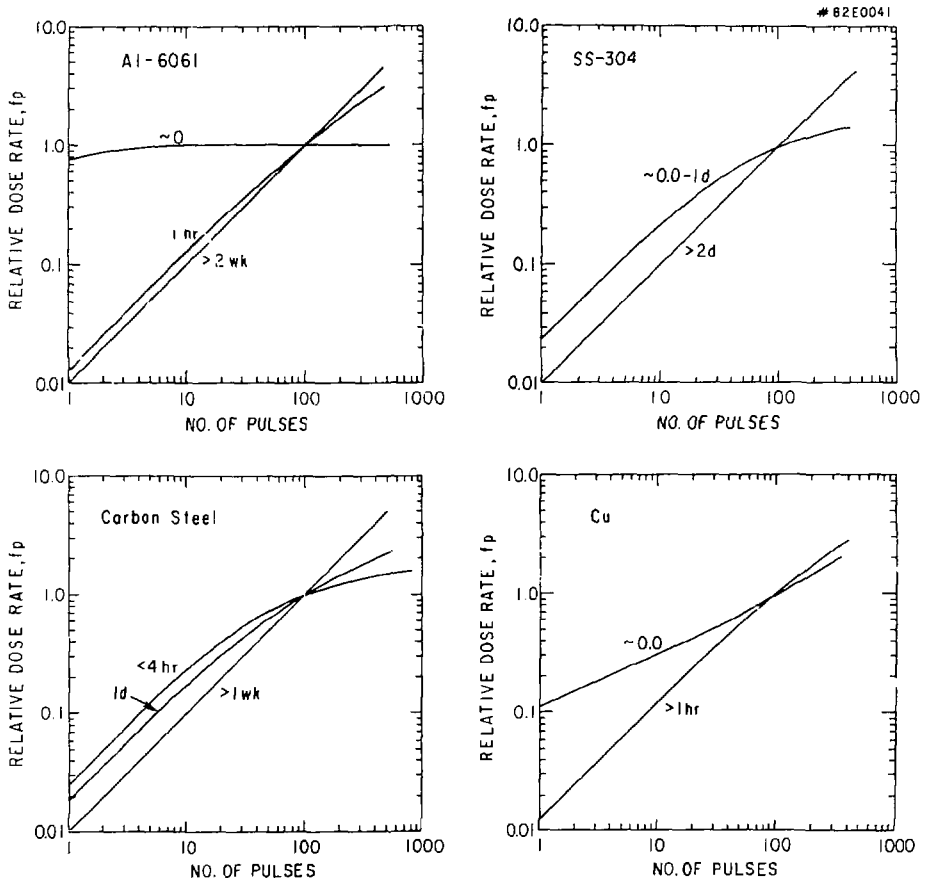

Fig. 32. Relative dose rate as a function of number of pulses, S10 spectrum.

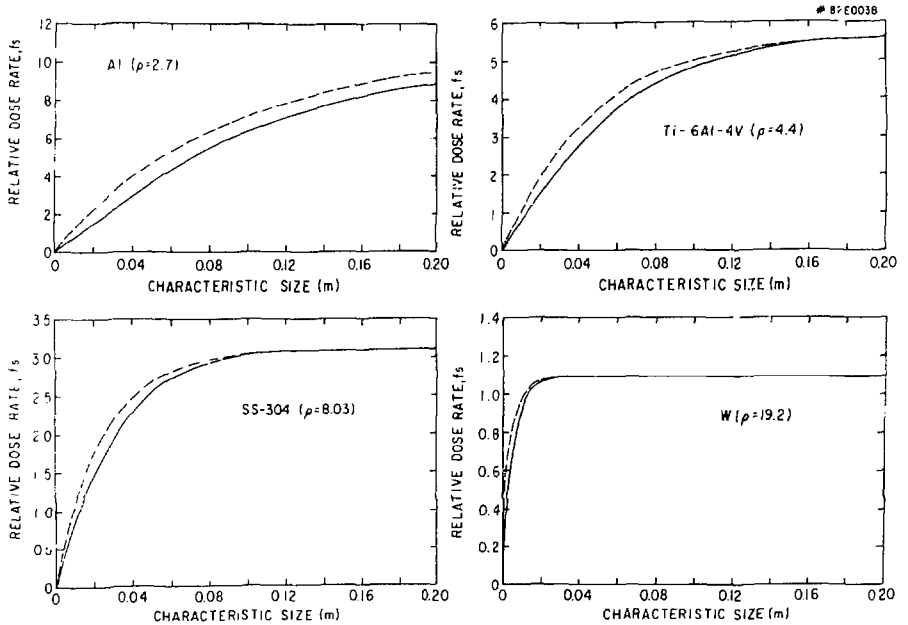

Fig. 33. Relative dose rate as a function of sample characteristic size.

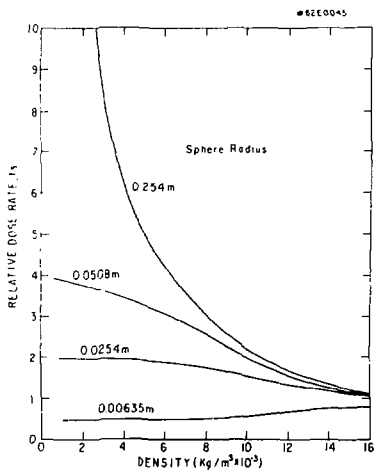

Fig. 34. Relative dose rate as a function of material density. Spheres, normalization reference = 0.0127-m-radius sphere.

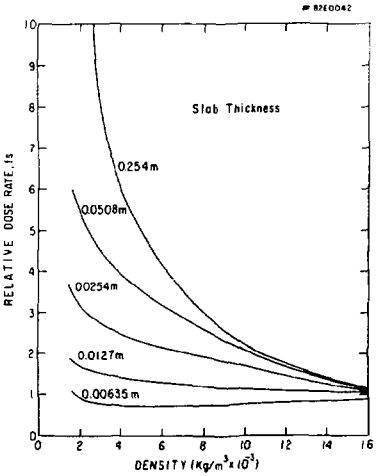

Fig. 35. Relative dose rate as a function of material density. Infinite slabs, normalization reference = 0.0127-m-radius sphere.

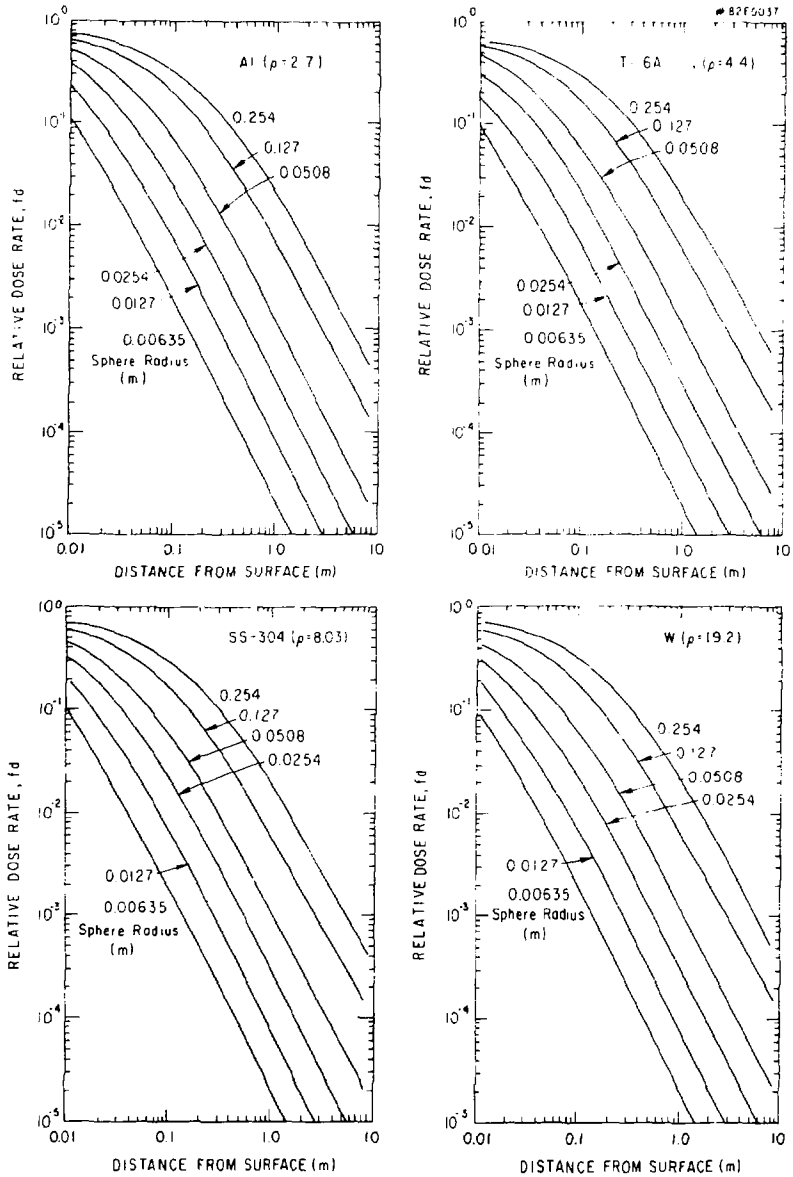

Fig. 36. Relative dose rate as a function of distance of observation from the surface of spheres of various radii.

TABLE 1. NOMINAL MATERIAL COMPOSITIONS

(A) Structural Materials

	SS-304	SS-316	A-286	PCA	Nitronic-33	Carbon Steel
C	0.0	0.06	0.04	0.06	0.0	0.25
Al	0.0	0.0	0.2	0.0	0.0	0.0
Si	0.0	1.0	0.5	0.5	0.0	0.35
P	0.0	0.0	0.0	0.0	0.0	0.04
S	0.0	0.0	0.0	0.0	0.0	0.05
Ti	0.0	0.0	2.1	0.3	0.0	0.0
Cr	19.0	17.0	14.75	14.0	18.0	0.20
Mn	2.0	2.0	1.25	1.88	13.0	1.0
Fe	69.0	65.44	54.16	64.76	65.62	97.10
Co	0.0	0.0	0.0	0.0	0.0	0.0
Ni	10.0	12.0	25.5	16.5	3.0	0.25
Cu	0.0	0.0	0.0	0.0	0.0	0.35
Mo	0.0	2.5	1.25	2.0	0.0	0.06
Pb	0.0	0.0	0.0	0.0	0.0	0.35
Density $kg/m^3 \cdot 10^{-3}$	8.03	7.92	7.92	7.92	7.75	8.03

(B) Structural Materials

	Ti-6242S	Vanstar-7	Nb-5Mo-1Zr	9Cr-1Mo	LRO-15
C	0.0	0.054	0.0	0.1	0.0
Al	6.0	0.0	0.0	0.0	0.0
Si	0.09	0.0	0.0	0.2	0.0
P	0.0	0.0	0.0	0.02	0.0
S	0.0	0.0	0.0	0.01	0.0
Ti	86.0	0.0	0.0	0.0	0.0
V	0.0	86.35	0.0	0.21	22.8
Cr	0.0	9.0	.0	8.5	0.0
Mn	0.0	0.0	0.0	0.4	0.0
Fe	0.0	3.3	0.0	89.43	36.1
Co	0.0	0.0	0.0	0.0	21.4
Ni	0.0	0.0	94.0	0.1	19.7
Zr	4.0	1.3	1.0	0.08	0.0
Nb	2.0	0.0	0.0	0.95	0.0
Mo	0.0	0.0	5.0	0.0	0.0
Sn	2.0	0.0	0.0	0.0	0.0
Density	4.5	6.3	8.6	7.9	7.8

(C) Structure Materials

	Al	Al-6061	Ti-6Al-4V
Mg	0.0	1.0	0.0
Al	100.0	97.92	6.0
Si	0.0	0.6	0.0
Ti	0.	0.0	90.0
V	0.0	0.0	4.0
Cr	0.0	0.2	0.0
Mn	0.0	0.0	0.0
Fe	0.0	0.0	0.0
Ni	0.0	0.0	0.0
Cu	0.0	0.28	0.0
Density	2.7	2.7	4.4

(D) Bellow, Protective Plate, Surface Pumping and Joint Materials

	Inconel 625	Inconel x 750	Constantan	Nimonic 90	Hi-Velcro
Be	0.0	0.0	0.0	0.0	0.005
C	0.05	0.04	0.0	0.0	0.054
Al	0.2	0.7	0.0	1.5	0.032
Si	0.3	0.25	0.0	0.5	0.634
P	0.008	0.0	0.0	0.0	0.016
S	0.008	0.005	0.0	0.0	0.017
Ti	0.2	2.5	0.0	2.5	0.115
Cr	22.0	16.0	0.0	19.5	19.378
Mn	0.25	0.5	0.0	0.5	1.101
Fe	2.5	7.0	0.0	1.0	59.278
Co	0.05	0.05	0.0	18.0	5.006
Ni	61.734	71.705	45.0	56.27	13.025
Cu	0.0	0.25	55.0	0.1	0.217
Zr	0.0	0.0	0.0	0.07	0.0
Nb	3.7	1.0	0.0	0.0	0.046
Mo	9.0	0.0	0.0	0.0	1.076
Density	8.44	8.25	8.93	8.18	8.10

(E) Surface Treatment Material, Brazes and Solders

	Yellow Brass	Cu-Sn	Cu-Ag	Wiping Solder	Soft Solder
Al	0.0	0.0	0.0	0.0	0.003
P	0.0	0.0	5.0	0.0	0.0
Fe	0.03	0.0	0.0	0.0	0.01
Ni	0.0	0.0	0.0	0.0	0.0
Cu	65.0	88.0	80.0	0.0	0.04
Zn	34.77	2.0	0.0	0.0	0.003
Ag	0.0	0.0	15.0	0.0	0.0
Sn	0.0	10.0	0.0	39.8	20.0
Sb	0.0	0.0	0.0	0.2	0.25
Pb	0.2	0.0	0.0	60.0	79.574
Bi	0.0	0.0	0.0	0.0	0.12
Density	8.47	8.2	8.87	9.3	10.2

(F) Coil, Ceramic Breaks and Limiter Materials

	Cu	Al_2O_3	Ti C	Mo	W
C	0.0	0.0	20.0	0.0	0.0
O	0.0	47.06	0.0	0.0	0.0
Al	0.0	52.94	0.0	0.0	0.0
Ti	0.0	0.0	80.0	0.0	0.0
Cu	100.0	0.0	0.0	0.0	0.0
Mo	0.0	0.0	0.0	100.0	0.0
W	0.0	0.0	0.0	0.0	100.0
Density	8.93	3.9	4.25	10.2	19.2

(G) Window Materials

	$Mg F_2$	$Si O_2$	Ag Cl	ZnSe
O	0.0	53.26	0.0	0.0
F	61.0	0.0	0.0	0.0
Mg	39.0	0.0	0.0	0.0
Si	0.0	46.74	0.0	0.0
Cl	0.0	0.0	24.74	0.0
Zn	0.0	0.0	0.0	45.3
Se	0.0	0.0	0.0	54.7
Ag	0.0	0.0	75.26	0.0
Density	2.5	2.65	5.56	5.42

TABLE 2

Relative activities for a standard SS-304 sample irradiated by 100 typical TFTR pulses.

See Section II, page 11 for the details of the weighting spectrum.

RELATIVE ACTIVITY FOR SS-304LN

PULSING SCENARIO INDEX = 4, WEIGHTING SPECTRUM INDEX = 2

ISOTOPE	0.0	1 HR	4 HR	1 D	2 D	1 WK	2 WK	2 MO	6 MO	1 YR	2 YR	5 YR
TI- 51	0.0012	0.0000	0.0000	0.0000	0.0000	0.0000	0.0000	0.0000	0.0000	0.0000	0.0000	0.0000
V- 49	0.0030	0.0000	0.0000	0.0005	0.0015	0.0017	0.0020	0.0057	0.0057	0.0044	0.0027	0.0006
V- 52	0.5076	0.0000	0.0000	0.0000	0.0000	0.0000	0.0000	0.0000	0.0000	0.0000	0.0000	0.0000
V- 53	0.0430	0.0000	0.0000	0.0000	0.0000	0.0000	0.0000	0.0000	0.0000	0.0000	0.0000	0.0000
V- 54	0.0190	0.0000	0.0000	0.0000	0.0000	0.0000	0.0000	0.0000	0.0000	0.0000	0.0000	0.0000
CR- 49	0.0015	0.0007	0.0001	0.0000	0.0000	0.0000	0.0000	0.0000	0.0000	0.0000	0.0000	0.0000
CR- 51	0.0059	0.0077	0.0173	0.3158	1.0000	1.0000	1.0000	1.0000	0.0635	0.0007	0.0000	0.0000
CR- 55	0.0237	0.0000	0.0000	0.0000	0.0000	0.0000	0.0000	0.0000	0.0000	0.0000	0.0000	0.0000
MN- 54	0.0004	0.0005	0.0011	0.0209	0.0677	0.0758	0.0890	0.2539	0.2487	0.1879	0.1081	0.0206
MN- 56	1.0000	1.0000	1.0000	0.0867	0.0004	0.0000	0.0000	0.0000	0.0000	0.0000	0.0000	0.0000
MN- 57	0.0437	0.0000	0.0000	0.0000	0.0000	0.0000	0.0000	0.0000	0.0000	0.0000	0.0000	0.0000
MN- 58	0.0038	0.0000	0.0000	0.0000	0.0000	0.0000	0.0000	0.0000	0.0000	0.0000	0.0000	0.0000
FE- 53	0.0084	0.0001	0.0000	0.0000	0.0000	0.0000	0.0000	0.0000	0.0000	0.0000	0.0000	0.0000
FE- 55	0.0012	0.0015	0.0034	0.0641	0.2078	0.2347	0.2782	0.8543	1.0000	1.0000	1.0000	1.0000
FE- 59	0.0000	0.0000	0.0000	0.0005	0.0017	0.0018	0.0019	0.0029	0.0006	0.0000	0.0000	0.0000
CO- 56	0.0000	0.0000	0.0000	0.0001	0.0003	0.0003	0.0004	0.0008	0.0003	0.0001	0.0000	0.0000
CO- 57	0.0031	0.0002	0.0004	0.0071	0.0239	0.0281	0.0330	0.0528	0.0873	0.0619	0.0315	0.0041
CO- 58	0.0010	0.0014	0.0035	0.0836	0.2831	0.3086	0.3433	0.6915	0.2730	0.0508	0.0018	0.0000
CO- 58M	0.1137	0.1379	0.2456	1.0000	0.5218	0.0001	0.0000	0.0000	0.0000	0.0000	0.0000	0.0000
CO- 60	0.0000	0.0000	0.0000	0.0003	0.0011	0.0013	0.0015	0.0047	0.0058	0.0062	0.0070	0.0102
CO- 61	0.0023	0.0020	0.0013	0.0000	0.0000	0.0000	0.0000	0.0000	0.0000	0.0000	0.0000	0.0000
CO- 62	0.0028	0.0002	0.0000	0.0000	0.0000	0.0000	0.0000	0.0000	0.0000	0.0000	0.0000	0.0000
CO- 63	0.0003	0.0000	0.0000	0.0000	0.0000	0.0000	0.0000	0.0000	0.0000	0.0000	0.0000	0.0000
CO- 64	0.0596	0.0000	0.0000	0.0000	0.0000	0.0000	0.0000	0.0000	0.0000	0.0000	0.0000	0.0000
NI- 57	0.0034	0.0043	0.0092	0.1167	0.2390	0.0271	0.0013	0.0000	0.0000	0.0000	0.0000	0.0000
NI- 63	0.0000	0.0000	0.0000	0.0000	0.0000	0.0000	0.0000	0.0001	0.0001	0.0001	0.0001	0.0003

RELATIVE ACTIVITY FOR SS-304LN

PULSING SCENARIO INDEX = 4, WEIGHTING SPECTRUM INDEX = 3

ISOTOPE	0.0	1 HR	4 HR	1 D	2 D	1 WK	2 WK	2 MO	6 MO	1 YR	2 YR	5 YR
TI- 51	0.0006	0.0000	0.0000	0.0000	0.0000	0.0000	0.0000	0.0000	0.0000	0.0000	0.0000	0.0000
V- 49	0.0000	0.0000	0.0000	0.0003	0.0009	0.0011	0.0012	0.0035	0.0051	0.0040	0.0024	0.0005
V- 52	0.2691	0.0000	0.0000	0.0000	0.0000	0.0000	0.0000	0.0000	0.0000	0.0000	0.0000	0.0000
V- 53	0.0216	0.0000	0.0000	0.0000	0.0000	0.0000	0.0000	0.0000	0.0000	0.0000	0.0000	0.0000
V- 54	0.0043	0.0000	0.0000	0.0000	0.0000	0.0000	0.0000	0.0000	0.0000	0.0000	0.0000	0.0000
CR- 49	0.0007	0.0003	0.0000	0.0000	0.0000	0.0000	0.0000	0.0000	0.0000	0.0000	0.0000	0.0000
CR- 51	0.0045	0.0058	0.0131	0.3806	1.0000	1.0000	1.0000	1.0000	0.0923	0.0010	0.0000	0.0000
CR- 55	0.0120	0.0000	0.0000	0.0000	0.0000	0.0000	0.0000	0.0000	0.0000	0.0000	0.0000	0.0000
MN- 54	0.0002	0.0003	0.0006	0.0181	0.0487	0.0546	0.0641	0.1829	0.2602	0.1966	0.1131	0.0215
MN- 56	1.0000	1.0000	1.0000	0.1381	0.0006	0.0000	0.0000	0.0000	0.0000	0.0000	0.0000	0.0000
MN- 57	0.0207	0.0000	0.0000	0.0000	0.0000	0.0000	0.0000	0.0000	0.0000	0.0000	0.0000	0.0000
MN- 58	0.0018	0.0000	0.0000	0.0000	0.0000	0.0000	0.0000	0.0000	0.0000	0.0000	0.0000	0.0000
FE- 53	0.0038	0.0000	0.0000	0.0000	0.0000	0.0000	0.0000	0.0000	0.0000	0.0000	0.0000	0.0000
FE- 55	0.0006	0.0008	0.0018	0.0531	0.1431	0.1616	0.1915	0.5861	1.0000	1.0000	1.0000	1.0000
FE- 59	0.0000	0.0001	0.0001	0.0033	0.0089	0.0093	0.0099	0.0154	0.0044	0.0003	0.0000	0.0000
CO- 56	0.0000	0.0000	0.0000	0.0001	0.0002	0.0002	0.0002	0.0005	0.0003	0.0001	0.0000	0.0000
CO- 57	0.0001	0.0001	0.0002	0.0054	0.0149	0.0175	0.0206	0.0574	0.0789	0.0560	0.0284	0.0037
CC- 58	0.0006	0.0009	0.0022	0.0836	0.2349	0.2560	0.2848	0.5738	0.3290	0.0613	0.0022	0.0000
CO- 58M	0.0714	0.0865	0.1541	1.0000	0.4330	0.0001	0.0000	0.0000	0.0000	0.0000	0.0000	0.0000
CO- 60	0.0000	0.0000	0.0000	0.0003	0.0008	0.0009	0.0010	0.0032	0.0058	0.0061	0.0070	0.0101
CO- 61	0.0011	0.0010	0.0006	0.0000	0.0000	0.0000	0.0000	0.0000	0.0000	0.0000	0.0000	0.0000
CO- 62	0.0010	0.0001	0.0000	0.0000	0.0000	0.0000	0.0000	0.0000	0.0000	0.0000	0.0000	0.0000
CO- 63	0.0001	0.0000	0.0000	0.0000	0.0000	0.0000	0.0000	0.0000	0.0000	0.000	0.0000	0.0000
CO- 64	0.0282	0.0000	0.0000	0.0000	0.0000	0.0000	0.0000	0.0000	0.0000	0.0000	0.0000	0.0000
NI- 57	0.0015	0.0020	0.0042	0.0849	0.1443	0.0163	0.0008	0.0000	0.0000	0.0000	0.0000	0.0000
NI- 63	0.0000	0.0000	0.0000	0.0000	0.0000	0.0000	0.0001	0.0002	0.0003	0.0003	0.0004	0.0005

RELATIVE ACTIVITY FOR SS-304LN

PULSING SCENARIO INDEX = 4, WEIGHTING SPECTRUM INDEX = 4

ISOTOPE	0.0	1 HR	4 HR	1 D	2 D	1 WK	2 WK	2 MO	6 MO	1 YR	2 YR	5 YR
TI- 51	0.0093	0.0096	0.0000	0.0000	0.0000	0.0000	0.0000	0.0000	0.0000	0.0000	0.0000	0.0000
V- 49	0.0030	0.0006	0.0000	0.0001	0.0004	0.0005	0.0006	0.0017	0.0044	0.0034	0.0020	0.0004
V- 52	0.2191	0.0000	0.0000	0.0000	0.0000	0.0000	0.0000	0.0000	0.0000	0.0000	0.0000	0.0000
V- 53	0.0137	0.0000	0.0000	0.0000	0.0000	0.0000	0.0000	0.0000	0.0000	0.0000	0.0000	0.0000
V- 54	0.0021	0.0000	0.0000	0.0000	0.0000	0.0000	0.0000	0.0000	0.0000	0.0000	0.0000	0.0000
CR- 49	0.0003	0.0001	0.0000	0.0000	0.0000	0.0000	0.0000	0.0000	0.0000	0.0000	0.0000	0.0000
CR- 51	0.0038	0.0056	0.0122	0.2717	1.0000	1.0000	1.0000	1.0000	0.1642	0.0078	0.0000	0.0000
CR- 55	0.0081	0.0000	0.0000	0.0000	0.0000	0.0000	0.0000	0.0000	0.0000	0.0000	0.0000	0.0000
MN- 54	0.0002	0.0002	0.0005	0.0132	0.0498	0.0558	0.0655	0.1869	0.4733	0.3576	0.2057	0.0392
MN- 56	1.0000	1.0000	1.0000	0.1149	0.0007	0.0000	0.0000	0.0000	0.0000	0.0000	0.0000	0.0000
MN- 57	0.0139	0.0000	0.0000	0.0000	0.0000	0.0000	0.0000	0.0000	0.0000	0.0000	0.0000	0.0000
MN- 58	0.0009	0.0000	0.0000	0.0000	0.0000	0.0000	0.0000	0.0000	0.0000	0.0000	0.0000	0.0000
FE- 53	0.0011	0.0000	0.0000	0.0000	0.0000	0.0000	0.0000	0.0000	0.0000	0.0000	0.0000	0.0000
FE- 55	0.0003	0.0004	0.0009	0.0213	0.0804	0.0908	0.1076	0.3292	1.0000	1.0000	1.0000	1.0000
FE- 59	0.0030	0.0001	0.0001	0.0033	0.0121	0.0127	0.0136	0.0210	0.0107	0.0007	0.0000	0.0000
CO- 56	0.0000	0.0000	0.0000	0.0000	0.0001	0.0001	0.0001	0.0002	0.0002	0.0000	0.0000	0.0000
CO- 57	0.0000	0.0000	0.0001	0.0020	0.0077	0.0089	0.0105	0.0295	0.0718	0.0509	0.0259	0.0034
CO- 58	0.0008	0.0011	0.0026	0.0836	0.3291	0.3587	0.3950	0.8039	0.8205	0.1528	0.0055	0.0000
CO- 58M	0.0857	0.1039	0.1852	1.0000	0.6065	0.0001	0.0000	0.0000	0.0000	0.0000	0.0000	0.0000
CO- 60	0.0040	0.0000	0.0000	0.0002	0.0007	0.0007	0.0009	0.0027	0.0086	0.0092	0.0104	0.0152
CO- 61	0.0007	0.0006	0.0004	0.0000	0.0000	0.0000	0.0000	0.0000	0.0000	0.0000	0.0000	0.0000
CO- 62	0.0007	0.0000	0.0000	0.0000	0.0000	0.0000	0.0000	0.0000	0.0000	0.0000	0.0000	0.0000
CO- 64	0.0127	0.0000	0.0000	0.0000	0.0000	0.0000	0.0000	0.0000	0.0000	0.0000	0.0000	0.0000
NI- 57	0.0005	0.0007	0.0015	0.0248	0.0591	0.0067	0.0003	0.0000	0.0000	0.0000	0.0000	0.0000
NI- 63	0.0000	0.0000	0.0000	0.0000	0.0001	0.0001	0.0001	0.0002	0.0008	0.0009	0.0012	0.0025

RELATIVE ACTIVITY FOR SS-304LN

PULSING SCENARIO INDEX = 4, WEIGHTING SPECTRUM INDEX = 5

ISOTOPE	0.0	1 HR	4 HR	1 D	2 D	1 WK	2 WK	2 MO	6 MO	1 YR	2 YR	5 YR
TI- 51	0.0002	0.0000	0.0000	0.0000	0.0000	0.0000	0.0000	0.0000	0.0000	0.0000	0.0000	0.0000
V- 49	0.0000	0.0000	0.0000	0.0001	0.0003	0.0004	0.0004	0.0013	0.0039	0.0030	0.0018	0.0024
V- 52	0.1928	0.0000	0.0000	0.0000	0.0000	0.0000	0.0000	0.0000	0.0000	0.0000	0.0000	0.0000
V- 53	0.0114	0.0000	0.0000	0.0000	0.0000	0.0000	0.0000	0.0000	0.0000	0.0000	0.0000	0.0000
V- 54	0.0016	0.0000	0.0000	0.0000	0.0000	0.0000	0.0000	0.0000	0.0000	0.0000	0.0000	0.0000
CR- 49	0.0001	0.0001	0.0000	0.0000	0.0000	0.0000	0.0000	0.0000	0.0001	0.0000	0.0000	0.0000
CR- 51	0.0038	0.0050	0.0112	0.2879	1.0000	1.0000	1.0000	1.0000	0.1985	0.0022	0.0000	0.0000
CR- 55	0.0068	0.0000	0.0000	0.0000	0.0000	0.0000	0.0000	0.0000	0.0000	0.0000	0.0000	0.0000
MN- 54	0.0002	0.0002	0.0005	0.0126	0.0448	0.0502	0.0589	0.1682	0.5148	0.3890	0.2238	0.0426
MN- 56	1.0000	1.0000	1.0000	0.1218	0.0007	0.0000	0.0000	0.0000	0.0000	0.0000	0.0000	0.0000
MN- 57	0.0117	0.0000	0.0000	0.0000	0.0000	0.0000	0.0000	0.0000	0.0000	0.0000	0.0000	0.0000
MN- 58	0.0007	0.0000	0.0000	0.0000	0.0000	0.0000	0.0000	0.0000	0.0000	0.0000	0.0000	0.0000
FE- 53	0.0008	0.0000	0.0000	0.0000	0.0000	0.0000	0.0000	0.0000	0.0000	0.0000	0.0000	0.0000
FE- 55	0.0002	0.0003	0.0007	0.0187	0.0665	0.0751	0.0890	0.2724	1.0000	1.0000	1.0000	1.0000
FE- 59	0.0000	0.0001	0.0001	0.0037	0.0128	0.0135	0.0144	0.0222	0.0138	0.0009	0.0000	0.0000
CO- 56	0.0030	0.0000	0.0000	0.0000	0.0000	0.0000	0.0001	0.0001	0.0002	0.0000	0.0000	0.0000
CO- 57	0.0000	0.0000	0.0001	0.0016	0.0059	0.0068	0.0080	0.0224	0.0658	0.0467	0.0237	0.0031
CO- 58	0.0037	0.0010	0.0025	0.0836	0.3106	0.3385	0.3765	0.7585	0.9359	0.1742	0.0063	0.0000
CO- 58M	0.0809	0.0981	0.1747	1.0000	0.5723	0.0001	0.0000	0.0000	0.0000	0.0000	0.0000	0.0000
CO- 60	0.0000	0.0000	0.0000	0.0002	0.0006	0.0006	0.0007	0.0023	0.0089	0.0095	0.0107	0.0156
CO- 61	0.0006	0.0005	0.0003	0.0000	0.0000	0.0000	0.0000	0.0000	0.0000	0.0000	0.0000	0.0000
CO- 62	0.0005	0.0000	0.0000	0.0000	0.0000	0.0000	0.0000	0.0000	0.0000	0.0000	0.0000	0.0000
CO- 64	0.0097	0.0000	0.0000	0.0000	0.0000	0.0000	0.0000	0.0000	0.0000	0.0000	0.0000	0.0000
NI- 57	0.0004	0.0005	0.0011	0.0190	0.0426	0.0048	0.0002	0.0000	0.0000	0.0000	0.0000	0.0000
NI- 63	0.0000	0.0000	0.0000	0.0000	0.0001	0.0001	0.0001	0.0003	0.0010	0.0012	0.0015	0.0032

RELATIVE ACTIVITY FOR SS-304LN

PULSING SCENARIO INDEX = 4, WEIGHTING SPECTRUM INDEX = 6

ISOTOPE	0.0	1 HR	4 HR	1 D	2 D	1 WK	2 WK	2 MO	6 MO	1 YR	2 YR	5 YR
V- 49	0.0000	0.0000	0.0000	0.0000	0.0000	0.0000	0.0000	0.0000	0.0002	0.0001	0.0001	0.0000
V- 52	0.0194	0.0000	0.0000	0.0000	0.0000	0.0000	0.0000	0.0000	0.0000	0.0000	0.0000	0.0000
V- 53	0.0009	0.0000	0.0000	0.0000	0.0000	0.0000	0.0000	0.0000	0.0000	0.0000	0.0000	0.0000
CR- 51	0.0051	0.0067	0.0149	1.0000	1.0000	1.0000	1.0000	1.0000	0.2355	0.0025	0.0000	0.0000
CR- 55	0.0016	0.0000	0.0000	0.0000	0.0000	0.0000	0.0000	0.0000	0.0000	0.0000	0.0000	0.0000
MN- 54	0.0030	0.0000	0.0001	0.0037	0.0038	0.0043	0.0050	0.0143	0.0531	0.0378	0.0218	0.0041
MN- 56	1.0000	1.0000	1.0000	0.3173	0.0005	0.0000	0.0000	0.0000	0.0000	0.0000	0.0000	0.0000
MN- 57	0.0010	0.0000	0.0000	0.0000	0.0000	0.0000	0.0000	0.0000	0.0000	0.0000	0.0000	0.0000
FE- 55	0.0033	0.0004	0.0008	0.0569	0.0583	0.0658	0.0780	0.2387	1.0000	1.0000	1.0000	1.0000
FE- 59	0.0001	0.0001	0.0002	0.0106	0.0107	0.0112	0.0126	0.0186	0.0131	0.0008	0.0000	0.0000
CO- 57	0.0000	0.0000	0.0000	0.0002	0.0002	0.0002	0.0003	0.0008	0.0027	0.0019	0.0010	0.0001
CO- 58	0.0001	0.0001	0.0003	0.0287	0.0307	0.0335	0.0373	0.0751	0.1057	0.0197	0.0087	0.0000
CO- 58M	0.0107	0.0129	0.0230	0.3437	0.0566	0.0000	0.0000	0.0000	0.0000	0.0000	0.0000	0.0000
CO- 60	0.0000	0.0000	0.0000	0.0000	0.0000	0.0000	0.0000	0.0001	0.0006	0.0007	0.0008	0.0011
CO- 64	0.0005	0.0000	0.0000	0.0000	0.0000	0.0000	0.0000	0.0000	0.0000	0.0000	0.0000	0.0000
NI- 57	0.0000	0.0000	0.0000	0.0018	0.0011	0.0001	0.0000	0.0000	0.0000	0.0000	0.0000	0.0000
NI- 59	0.0000	0.0000	0.0000	0.0000	0.0000	0.0000	0.0000	0.0000	0.0000	0.0000	0.0001	0.0001
NI- 63	0.0000	0.0000	0.0000	0.0002	0.0002	0.0003	0.0003	0.0010	0.0044	0.0050	0.0064	0.0135

RELATIVE ACTIVITY FOR SS-304LN

PULSING SCENARIO INDEX = 4, WEIGHTING SPECTRUM INDEX = 8

ISOTOPE	0.0	1 HR	4 HR	1 D	2 D	1 WK	2 WK	2 MO	6 MO	1 YR	2 YR	5 YR
CR- 51	0.0042	0.0045	0.0056	0.0252	0.1532	0.2590	0.2328	0.1156	0.0186	0.0004	0.0000	0.0000
MN- 54	0.0012	0.0013	0.0016	0.0072	0.0447	0.0848	0.0894	0.1268	0.3142	0.4547	0.2846	0.0542
MN- 56	0.9912	0.8176	0.4589	0.0098	0.0001	0.0000	0.0000	0.0000	0.0000	0.0000	0.0000	0.0000
FE- 55	0.0013	0.0015	0.0018	0.0084	0.0522	0.0996	0.1062	0.1613	0.4799	1.0000	1.0000	1.0000
FE- 59	0.0001	0.0001	0.0001	0.0007	0.0040	0.0071	0.0068	0.0052	0.0026	0.0003	0.0000	0.0000
CO- 58	0.0091	0.0102	0.0142	0.0836	0.5427	1.0000	1.0000	1.0000	1.0000	0.3879	0.0141	0.0000
CO- 58M	1.0000	1.0000	1.0000	1.0000	1.0000	0.0002	0.0000	0.0000	0.0000	0.0000	0.0000	0.0000
CO- 60	0.0030	0.0000	0.0000	0.0000	0.0000	0.0000	0.0000	0.0000	0.0000	0.0001	0.0001	0.0001
CO- 61	0.0001	0.0001	0.0000	0.0000	0.0000	0.0000	0.0000	0.0000	0.0000	0.0000	0.0000	0.0000
NI- 63	0.0000	0.0000	0.0000	0.0000	0.0000	0.0000	0.0000	0.0001	0.0002	0.0005	0.0006	0.0012

RELATIVE ACTIVITY FOR SS-304LN

PULSING SCENARIO INDEX = 4, WEIGHTING SPECTRUM INDEX = 9

ISOTOPE	0.0	1 HR	4 HR	1 D	2 D	1 WK	2 WK	2 MO	6 MO	1 YR	2 YR	5 YR
CR- 51	0.0035	0.0046	0.0103	0.7272	1.0000	1.0000	1.0000	1.0000	0.2699	0.0030	0.0000	0.0000
MN- 54	0.0000	0.0000	0.0001	0.0067	0.0094	0.0105	0.0124	0.0353	0.1470	0.1111	0.0639	0.0122
MN- 56	1.0000	1.0000	1.0000	0.3352	0.0007	0.0000	0.0000	0.0000	0.0000	0.0000	0.0000	0.0000
FE- 55	0.0002	0.0002	0.0005	0.0347	0.0489	0.0552	0.0655	0.2003	1.0000	1.0000	1.0000	1.0000
FE- 59	0.0001	0.0001	0.0002	0.0144	0.0200	0.0219	0.0225	0.0347	0.0292	0.0019	0.0000	0.0000
CO- 58	0.0003	0.0004	0.0009	0.0836	0.1230	0.1340	0.1491	0.3003	0.5039	0.0938	0.0034	0.0000
CO- 58M	0.0294	0.0356	0.0635	1.0000	0.2266	0.0000	0.0000	0.0000	0.0000	0.0000	0.0000	0.0000
NI- 63	0.0000	0.0000	0.0000	0.0000	0.0001	0.0001	0.0001	0.0003	0.0015	0.0017	0.0022	0.0047

RELATIVE ACTIVITY FOR SS-304LN

PULSING SCENARIO INDEX = 4, WEIGHTING SPECTRUM INDEX = 10

ISOTOPE	0.0	1 HR	4 HR	1 D	2 D	1 WK	2 WK	2 MO	6 MO	1 YR	2 YR	5 YR
CR- 51	0.0052	0.0068	0.0152	1.0000	1.0000	1.0000	1.0000	1.0000	0.2351	0.0026	0.0000	0.0000
MN- 54	0.0000	0.0000	0.0000	0.0002	0.0002	0.0003	0.0003	0.0009	0.0033	0.0025	0.0014	0.0003
MN- 56	1.0000	1.0000	1.0000	0.3126	0.0005	0.0000	0.0000	0.0000	0.0000	0.0000	0.0000	0.0000
FE- 55	0.0033	0.0004	0.0008	0.0548	0.0561	0.0634	0.0751	0.2299	1.0000	1.0000	1.0000	1.0000
FE- 59	0.0001	0.0001	0.0002	0.0106	0.0107	0.0112	0.0120	0.0186	0.0136	0.0009	0.0000	0.0000
CO- 58	0.0000	0.0000	0.0000	0.0032	0.0034	0.0037	0.0041	0.0082	0.0120	0.0022	0.0001	0.0000
CO- 58M	0.0012	0.0014	0.0026	0.0377	0.0062	0.0000	0.0000	0.0000	0.0000	0.0000	0.0000	0.0000
NI- 59	0.0000	0.0000	0.0000	0.0000	0.0000	0.0000	0.0000	0.0000	0.0000	0.0000	0.0001	0.0001
NI- 63	0.0000	0.0000	0.0000	0.0002	0.0002	0.0003	0.0003	0.0010	0.0045	0.0051	0.0066	0.0139

TABLE 3. Listing of Important Isotopes Contributing to Activity

Material	1 hour	1 day	1 week	6 months	1 year	2 years	5 years
Cr-Fe-Ni Alloy (1)	Mn-56 Co-58m	Mn-56 Co-58m	Cr-51 Co-58	Co-58 Mn-54	Mn-54 Co-58	Mn-54 Fe-55	Mn-54 Fe-55
		Cr-51	Fe-55	Fe-55	Fe-55	Co-60	Co-60
		Ni-57*	Mo-99	Co-57*	Co-57*		
		Mo-99	Tc-99m				
		Tc-99m					
Ni-based Alloy (2)	Mn-56 Co-58m	Cr-51 Co-58m	Cr-51 Co-58	Co-58 Cr-51	Co-58 Mn-54	Mn-54 Co-60	Co-60 Fe-55
		Mo-99	Co-60	Fe-55	Fe-55	Co-58	Co-57*
		Tc-99m	Mo-99	Co-57*	Co-57*	Fe-55	Ni-63
			Tc-99m	Co-60	Co-60 Ni-63	Co-57* Ni-63	

(1) For SS-304, SS-316, A-286, Carbon Steel, Nitromic-33, PCA.

(2) For Inconel 625, x750, Nimonic-90, Hi-Velcro, LRO-15.

* DT ONLY.

TABLE 3 - (CONT.)

Material	1 hour	1 day	1 week	6 months	1 year	2 years	5 years
Ti-alloy (3)	Sc-47	Sc-47	Sc-47	Ca-45*	Ca-45*	Ca-45*	Sc-46
	Sc-48*	Sc-48*	Sc-48*	Sc-46	Sc-46	Sc-46	Ca-45*
	Sc-49*	Na-24*					
	Ti-45*						
	Na-24*						
Vanstar-7	Mn-56	Sc-48	Sc-48	Cr-51	Fe-55	Fe-55	Fe-55
	Sc-48	Cr-51	Zr-89	Fe-55	V-49	V-49	Mn-54
	Y-93	Zr-89	Cr-51	V-49	Mn-54	Mn-54	
	Cr-51						
	Zr-93						
	Zr-89						
Al-alloy (4)	Na-24*	Na-24*	Na-24*	Al-26*	Al-26*	Al-26*	Al-26*
	Mg-27	Cu-64	Cn-64*	Cr-51	Co-60*	V-49*	Ni-63
	Cu-64			Co-60*	V-49*	Ni-63	Co-60*
					Ni-63	Co-60*	

(3) For Ti-6Al-4V, Tic, Ti-6242S.

(4) For Al, Al-6061, Al_2O_3

TABLE 3 - (CONT.)

Material	1 hour	1 day	1 week	6 months	1 year	2 years	5 years
Nb-5Mo-1Zr	Mo-99	Mo-99	Mo-99	Nb-93m	Nb-93m	Nb-93m	Nb-93m
	Tc-99m	Tc-99m	Tc-99m	Zr-95	Zr-95		
	Nb-94m	Nb-92m*	Nb-93m	Nb-95	Nb-95		
	Tc-101						
	Mo-101		Nb-92m*				
	Mo-93m						
	Nb-92m*						
Mo	Mo-99	Mo-99	Mo-99	Nb-92m	Tc-99	Tc-99	Tc-99
	Tc-99m	Tc-99m	Tc-99m	Nb-91m*	Zr-95*	Y-88	Nb-93m
	Mo-101	Mo-93m		Nb-95*	Y-88*		
	Tc-101			Zr-95*	Zr-88*		
	Mo-93m			Y-88*			
	Mo-91*			Zr-88*			
W	W-187	W-187	W-187	W-185	W-185	W-185	W-185
			W-185	W-181*	W-181*	W-181*	W-181*
			W-181*				

TABLE 3 - (CONT.)

Material	1 hour	1 day	1 week	6 months	1 year	2 years	5 years
Cu	Cu-64	Cu-64	Cu-64	Co-60*	Co-60*	Co-60*	Co-60*
	Cu-62*		Co-60*	Ni-63	Ni-63	Ni-63	Ni-63
Yellow Brass	Cu-64	Cu-64	Zn-65	Zn-65	Zn-65	Zn-65	Ni-63
	Zn-69		Cu-64	Co-60*	Co-60*	Ni-63	Co-60*
	Zn-63*					Co-60*	Zn-65
Cu-Sn	Cu-64	Cu-64	Sn-117m	Sn-119m	Sn-119m	Sn-119m	Ni-63
	Cu-62*		Cu-64	Sn-113	Ni-63	Ni-63	Sn-119m
			Sn-125	Zn-65	Zn-65	Sb-125	Sb-125
			Sn-119m	Co-60*	Sb-125	Zn-65	Co-60*
					Co-60*	Co-60*	
Cu-Ag	Cu-64	Cu-64	Ag-110m	Ag-110m	Ag-110m	Ag-110m	Ag-110m
	Si-31		Ag-106m		Co-60*	Co-60*	Co-60*
							Ni-63
							Ag-108m

TABLE 3 - (CONT.)

Material	1 hour	1 day	1 week	6 months	1 year	2 years	5 years
Solder	Sn-121	Sn-121	Sn-117m	Sn-119	Sn-119m	Sn-119m	Sn-119m
	Sn-117m	Sn-117m	Sn-125	Sn-113	Sb-125	Sb-125	Sb-125
	Sn-123m	Sb-122	Pb-203	Sn-123	Sn-123	Sn-123	
	Sn-113m	Pb-203	Sn-119				
	Sn-111	In-111					
	Pb-203						
MgF_2	F-18*	Na-24	Na-24				
	Na-24						
	Mg-27						
SiO_2	Si-31	Si-31	Si-31				
	Mg-27						
	Al-29						
AgCl	Ag-106	Ag-106m	Ag-106m	Ag-110m	Ag-110m	Ag-110m	Ag-110m
	Ag-106m	Ag-110m	Ag-110m				Ag-108m
	Ag-110m	P-32	P-32				
		Pd-109					

TABLE 3 - (CONT.)

Material	1 hour	1 day	1 week	6 months	1 year	2 years	5 years
ZnSe	Se-81	Cu-64	As-77*	Zn-65	Zn-65	Zn-65	Zn-65
	Se-81m	Ge-77*	Zn-65	Se-75	Se-75		
	Cu-64	As-77*	Se-75				
	Zn-63	Zn-69	Cu-67				
	Zn-69	Zn-69m	As-74				
	Br-83						